Jeon *et al. Soft Sci.* **2025**, *5*, 1
DOI: 10.20517/ss.2024.35

Soft Science

Review Article

Open Access

Check for updates

High-performance metal oxide TFTs for flexible displays: materials, fabrication, architecture, and applications

Seong-Pil Jeon[1,#], Jeong-Wan Jo[2,#], Dayul Nam[1], Yong-Hoon Kim[3,*], Sung Kyu Park[1,*]

[1]School of Intelligent Semiconductor Engineering, Chung-Ang University, Seoul 06974, Republic of Korea.
[2]Electrical Engineering Division, Department of Engineering, University of Cambridge, Cambridge CB3 0FA, UK.
[3]School of Advanced Materials Science and Engineering and SKKU Advanced Institute of Nanotechnology (SAINT), Sungkyunkwan University, Suwon 16419, Republic of Korea.
[#]Authors contributed equally.

[*]**Correspondence to:** Prof. Yong-Hoon Kim, School of Advanced Materials Science and Engineering and SKKU Advanced Institute of Nanotechnology (SAINT), Sungkyunkwan University, 2066, Seobu-ro, Jangan-gu, Suwon 16419, Republic of Korea. E-mail: yhkim76@skku.edu; Prof. Sung Kyu Park, School of Intelligent Semiconductor Engineering, Chung-Ang University, 84, Heukseok-ro, Dongjak-gu, Seoul 06974, Republic of Korea. E-mail: skpark@cau.ac.kr

How to cite this article: Jeon, S. P.; Jo, J. W.; Nam, D.; Kim, Y. H.; Park, S. K. High-performance metal oxide TFTs for flexible displays: materials, fabrication, architecture, and applications. *Soft Sci.* **2025**, *5*, 1. https://dx.doi.org/10.20517/ss.2024.35

Received: 29 Aug 2024 **First Decision:** 17 Oct 2024 **Revised:** 7 Nov 2024 **Accepted:** 15 Nov 2024 **Published:** 10 Jan 2025

Academic Editor: Carlo Massaroni **Copy Editor:** Pei-Yun Wang **Production Editor:** Pei-Yun Wang

Abstract

Flexible display technology is actively explored as a cornerstone of the next generation of wearables and soft electronics, set to revolutionize devices with its potential for lightweight, thin, and mechanically flexible features. Flexible thin-film transistors (TFTs) utilizing promising materials such as amorphous silicon (a-Si), low-temperature polysilicon (LTPS), metal oxides (MOs), and organic semiconductors are essential to enable flexible platforms. Among these, MO semiconductors stand out for flexible displays due to their high carrier mobility, low processing temperature requirements, excellent electrical uniformity, transparency to visible light, and cost-effectiveness. Furthermore, the maturity of MO TFT technology in the existing display industry and its compatibility with complementary-metal-oxide-semiconductor (CMOS) processes are driving active research toward integrated circuits for wearable electronics beyond display applications. Specifically, achieving both high mechanical flexibility and electrical performance in MO TFTs is crucial for implementing complex integrated circuits such as microprocessors and backplanes for ultra-high resolution augmented reality (AR)/virtual reality (VR) displays. Therefore, this review provides recent advances in high-mobility flexible MO TFTs, focusing on materials, fabrication processes, and device architecture engineering methods for implementing MO TFTs on flexible substrates, as well as strategies to reduce the impact of mechanical stress on MO TFTs. Next, MO TFT-based

display and integrated circuit applications for next-generation flexible and stretchable electronics are introduced and discussed. Finally, the review concludes with an outlook on the potential achievements and prospects of MO TFTs in the development of next-generation flexible display technologies.

Keywords: Flexible electronics, metal oxide, thin-film transistors, high-k dielectric, wearable devices, flexible devices

INTRODUCTION

Thin-film transistors (TFTs) are three-terminal semiconductor devices with a thin-film structure that act as switches in electronic circuits, controlling the flow of current and facilitating the operation of various electronic components. TFTs are currently the dominant technology for in-pixel switches and drivers in flat-panel displays, performing a critical function in active matrix (AM) displays, such as liquid crystal displays (LCDs) and active-matrix organic light-emitting diodes (AMOLEDs)[1-4]. Advances in TFT technology have aimed to reduce the carbon footprint while overcoming the limitations of conventional silicon-based transistors, such as limited form factor, difficulty in large-area processing, and high manufacturing costs[5-8]. As a result, TFTs have attracted significant interest for use in foldable, flexible and stretchable displays and other electronic products, potentially replacing traditional silicon complementary-metal-oxide-semiconductor (CMOS) circuits. TFTs are developed using various materials, including amorphous silicon (a-Si), polycrystalline silicon (poly-Si), metal oxides (MOs), and organic semiconductors[1,5,9,10]. Among these, MO semiconductors are particularly promising due to their advantages such as low cost, low process complexity and temperature, large area scalability, and higher carrier mobility compared to a-Si and organic materials[11-14]. In addition, MO TFTs offer greater resistance to mechanical stress than low-temperature polysilicon (LTPS) devices, making them ideal for next-generation flexible and stretchable electronics[12,15-17]. These advantages of MO TFTs have facilitated their successful commercialization in the display market, particularly through indium gallium zinc oxide (IGZO) TFT-based backplanes, which have driven significant growth and innovation in high-resolution organic light-emitting diode (OLED) panels since 2013[10,18,19]. With their transparency, flexibility, and high electron mobility, these MO TFTs have proven highly suitable for next-generation electronic devices, playing a crucial role in advancing flexible and transparent displays.

Flexible displays offer characteristics such as thinness, lightweight design, and durability, which allow them to be fabricated on curvilinear surfaces, enabling shape transformation. The history of flexible displays dates back to early innovations such as Polymer Vision's Readius in 2006, which used rollable e-paper, and Nokia's Morph concept in 2008, which envisioned a bendable and interactive mobile display. The development of thin, flexible OLED displays further expanded these possibilities. During the 2013 Consumer Electronics Show, Samsung introduced its "Youm" concept, which showcased flexible display prototypes, including a smartphone that folded outward into a tablet-sized display. The first commercial application of this technology appeared in the Galaxy Note Edge, with its curved OLED screen. In 2018, Royole released the first foldable smartphone, the Flexpai, followed by Samsung's Galaxy Fold in 2019, featuring an inward-folding Infinity Flex display. That same year, Huawei and Xiaomi also introduced their folding smartphones, signaling the growing maturity of flexible display technology and its impact on the smartphone market[20]. This wave of foldable devices underscored the maturation of flexible display technology and its potential for transforming the smartphone market. Since then, flexible displays, particularly flexible AMOLEDs, have achieved commercial success, driven by the popularization of high-resolution TVs, smartphones, and smart devices. Market research projected that shipments of flexible AMOLED displays would reach 335.7 million units by 2020, accounting for 52.0% of total AMOLED panel shipments, underscoring the growing market demand and technological advancements in this area[21].

Currently, along with the advancement of next-generation soft electronics, the development of MO TFT technology is accelerating to meet demands beyond flexible and transparent displays. This includes achieving higher resolution, lower power consumption, and accommodating new functionalities and form factors, marking a significant shift toward innovative applications such as foldable and wearable devices, automotive displays, and smart sensors[8,10,12,22,23]. MO TFTs play a key role not only in the advancement of displays, but also in the expansion into various flexible and stretchable electronic components for soft electronics. This includes applications such as efficient memory systems, flexible and stretchable circuits, sensors and advanced processors[24-34]. MO TFTs also highlight the transformative potential of next-generation Internet of Things (IoT) devices and advanced technologies such as artificial intelligence (AI) and neuromorphic computing[35-42]. In the rapidly evolving landscape of augmented reality (AR) and virtual reality (VR), the demand for high-performance display technologies continues to grow. MO TFTs have emerged as key components due to their exceptional transparency and low power consumption, making them indispensable for the realization of high-resolution backplane applications in AR/VR devices[43,44]. These TFTs not only enhance visual clarity, but also enable immersive user experiences by driving advances in display quality and efficiency. Furthermore, MO TFTs are increasingly valued for their unique capabilities in back-end-of-line (BEOL) processing and monolithic 3D (M3D) integration[45-48]. Their low processing temperatures, superior stability and low leakage characteristics allow seamless integration with existing silicon CMOS chips in BEOL processes, enabling higher transistor densities and more compact layouts. This compatibility not only improves the performance and efficiency of integrated circuits, but also opens new avenues for the development of advanced M3D architectures that promise significant advances in semiconductor technology.

Despite their critical role in advancing soft electronics, flexible MO TFTs face significant challenges due to inherent characteristics such as brittleness and limited electrical performance at low process temperatures. Balancing high electrical performance, reliability, and flexibility remains a complex task, particularly ensuring that these devices withstand mechanical stress and maintain functionality over extended bending cycles and varying bending radii. Furthermore, research is advancing beyond flexibility towards the development of stretchable MO TFTs, seen as key enablers for future applications such as wearable health monitors, electronic skin (e-skin), neuromorphic devices, and advanced human-machine interfaces[49-51]. This development focuses on novel materials and device architectures that maintain performance under large strains, often employing stretchable substrates combined with MO or organic semiconductors for electronic and mechanical robustness. Additionally, stretchable TFTs incorporate innovative geometries, such as serpentine or mesh structures, allowing deformation without sacrificing electrical properties, thus enhancing their potential in soft, stretchable electronics[51-54]. As a result, recent studies have focused extensively on improving the performance, processes, and structural design of flexible and stretchable MO TFT devices to increase mechanical stress resistance while minimizing electrical performance degradation and variability.

In this review, we investigate the substrate, materials, fabrication processes, device structures, and applications of high-performance flexible MO TFTs as shown in Figure 1. Firstly, in the substrate section, we classify the types of substrates for employing high-performance flexible MO TFTs into polymer, paper, and metal foil, and then describe the characteristics and types of each. Secondly, in the materials section, we focus on MO semiconductors and high-k dielectrics for achieving high-performance flexible TFTs. In the MO semiconductor subsection, we discuss the high mobility of indium tin zinc oxide (ITZO), ZnO:N, LiZnO, *etc.*, and multiple stack layers in detail. In the high-k dielectric subsection, we describe the impact and effects of polymer dielectrics and high-k dielectrics on the performance of flexible TFTs. Thirdly, in the fabrication process section, we examine the doping processes that significantly enhance the electrical

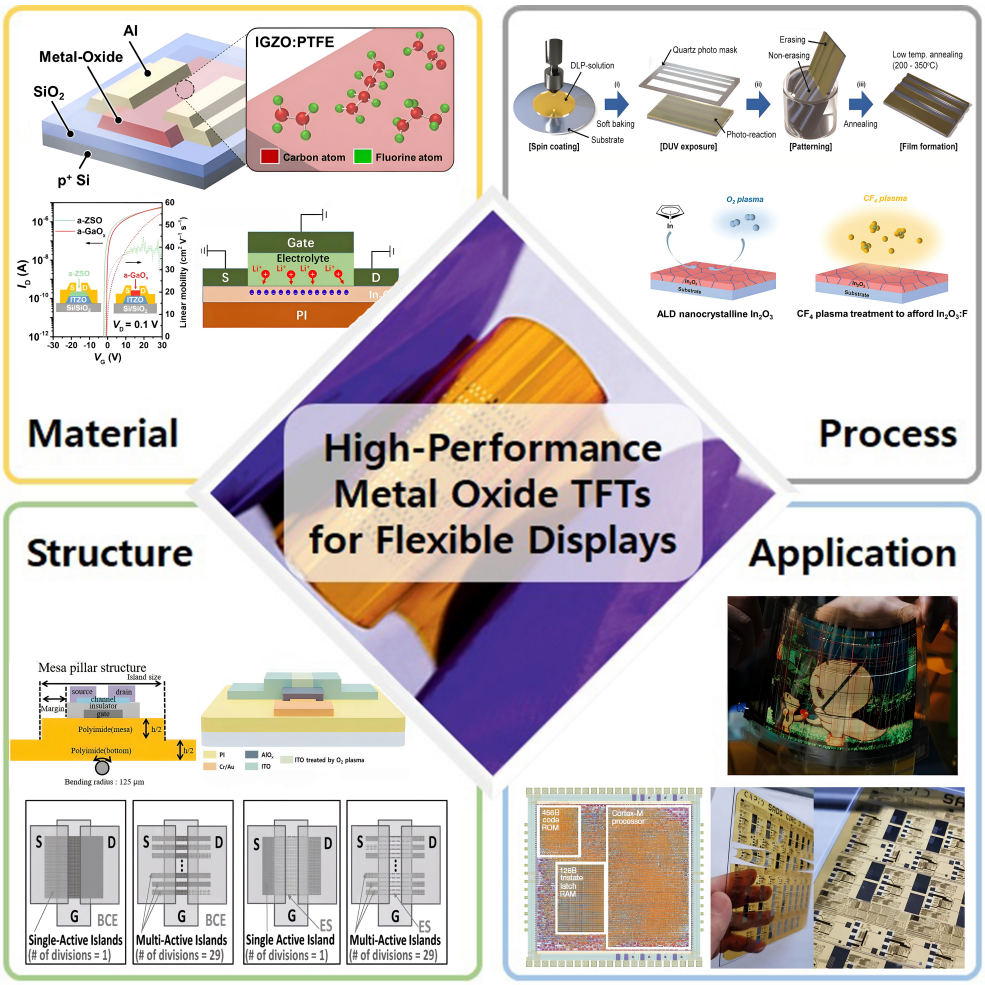

Figure 1. Schematic diagram illustrating approaches for high-performance MO TFTs in flexible display applications. MO: Metal oxide; TFTs: thin-film transistors.

performance of flexible MO TFTs. Doping with hydrogen, fluorine, nitrogen, and metal cations affects the electrical performance of flexible MO TFTs. These doping techniques not only improve electrical performance but are also compatible with the low-temperature fabrication required for flexible substrates. Consequently, these doping processes are beneficial in improving the electrical properties of MO TFTs for next-generation flexible electronic devices[55-60]. Fourthly, in the device structures section, we explore various innovative structures such as island structures, junctionless structures, and advanced electrode and channel layer architectures that enhance the flexibility of MO TFTs. These structural innovations play a crucial role in the development of flexible electronics that maintain high performance and mechanical stability in a wide range of wearable applications by ensuring consistent electrical performance despite significant mechanical deformation[33,61-67]. Fifthly, in the application section, we introduce applications of high-performance flexible TFTs, including displays and circuits that utilize high-performance flexible TFTs. Finally, we summarize the significant advances, remaining challenges, and potential future developments in flexible MO TFT technology.

VARIOUS SUBSTRATE OF FLEXIBLE MO TFT

To create flexible devices, it is essential to prepare bendable substrate materials, and oxide TFTs, which can be manufactured at low temperatures, are well-suited for use with flexible substrates. Many studies have explored flexible oxide-based TFTs, classified by the type of substrate material, such as polymer plastics, paper, and metal foils. In the development of flexible devices, the use of bendable substrate materials is a key requirement, as these substrates must maintain their structural integrity under mechanical deformation such as bending or stretching. Oxide TFTs processed at relatively low temperatures are particularly advantageous for integration with such flexible substrates. This compatibility with a low-temperature process allows oxide-based TFTs to be effectively utilized in various flexible electronic applications. Much research has been conducted on flexible oxide TFTs with the primary focus on the types of substrate materials that enable these devices to achieve high flexibility and performance. These studies often classify the substrates into three main groups: polymer plastics, paper sheets, and metal foils.

Polymeric materials

Polymeric materials offer numerous advantages, such as being flexible, stretchable, bendable, lightweight and highly transparent, making them appropriate materials for use in flexible substrates in various electronic applications[14,68,69]. These properties enable polymeric materials to support the development of advanced flexible electronics, including displays, sensors, and wearable devices. Amorphous oxide TFT technology, which can be processed at relatively low temperatures, is highly compatible with polymeric materials, allowing for scalable and cost-effective manufacture[12]. Among these materials, polyimide (PI) stands out as the most commonly used substrate for flexible oxide TFTs due to its excellent thermal stability, mechanical flexibility, and processability[70-73]. Other frequently used polymeric materials include polyethylene terephthalate (PET)[74-76], polyethylene naphthalate (PEN)[77-79], poly(vinyl alcohol) (PVA)[80], polydimethylsiloxane (PDMS)[52,81], polycarbonate (PC)[82], and polyether sulfone (PES)[83,84], each offering unique mechanical and chemical properties suitable for different applications. In addition, glass-fabric reinforced composite films are used as flexible plastic substrates, providing additional mechanical strength and stability while maintaining the flexibility needed for next-generation flexible electronics[85]. These materials combined with advancements in oxide-based TFT technology are driving innovation in flexible, lightweight, and durable electronics that can conform to various shapes and surfaces.

Paper sheets

Paper is an attractive alternative substrate for flexible electronics due to its low cost, renewable nature, and biodegradability. These substrates offer an eco-friendly solution compared to traditional plastics. Employing paper sheets in flexible oxide TFTs has potential in applications such as disposable electronics and smart packaging[86,87]. However, the rough surface and moisture absorption tendency of paper sheets create challenges to reliable fabrication and performance limiting their direct application in high-performance devices. To address these issues, surface treatments such as thin layers of silicon dioxide (SiO_2) deposited via plasma-enhanced chemical vapor deposition (PECVD)[88] or epoxy acrylate copolymer coatings are applied[89]. These coatings smooth surface of paper and act as moisture barriers improving suitability for flexible electronics. This allows paper-based devices to combine environmental sustainability with enhanced performance and durability.

Metal foils

Metal foils, including those made from gold, silver, copper, Hastelloy or aluminum, offer significant advantages in flexible electronics due to their excellent mechanical strength, ductility, and high thermal resistance. Unlike polymer plastics, metal foils can withstand a higher temperature process allowing for a broader range of fabrication techniques[90]. Their ability to bend with very small curvature radii makes them ideal for high-strain applications such as sensors integrated into advanced systems such as artificial skin[91].

One example is the work by Tang *et al.* who developed flexible MO TFT using GaO_x TFTs on 50-μm-thick metal foils[92]. These devices demonstrated impressive performance, uniformity, and stability. This study exhibits the potential of metal foil substrates in next-generation flexible device technologies, particularly in applications requiring flexibility and durability.

MATERIALS OF HIGH-PERFORMANCE FLEXIBLE MO TFT

High-performance flexible MO TFTs necessitate the use of sophisticated materials to simultaneously achieve superior electrical performance and exceptional mechanical stability. The active semiconductor layer is a charge transport layer, where charge carriers are generated and modulated. MOs such as indium oxide (In_2O_3), IGZO, and zinc oxide (ZnO) are widely used due to their high electron mobility, optical transparency, and environmental stability[11,93,94]. These materials can be doped with various elements to their electrical properties, improve carrier concentration, and enhance electrical performance. For example, doping with tin (Sn) in In_2O_3 [forming indium-tin-oxide (ITO)] increases carrier concentration, while doping with gallium (Ga) and zinc (Zn) in IGZO optimizes semiconductor properties and improves stability[55,95-97]. Multiple layers improved the performance of flexible MO TFTs. They are formed by combining different semiconductor materials to create interfaces that enhance efficient charge carrier transport. Selecting materials with complementary properties and multiple layers can significantly improve carrier mobility and reduce off-current, thereby enhancing electrical device performance. This approach minimizes energy loss and ensures that electronic devices operate with high efficiency and reliability over time[61,95,98-100]. The flexibility of the semiconductor layer is essential for maintaining device performance under mechanical stress such as bending and stretching. In flexible electronic devices, the semiconductor layer must withstand significant physical stress without degrading its electrical properties. MO semiconductors are inherently brittle due to their crystalline or amorphous structures. This brittleness makes them susceptible to cracking and fracture under mechanical deformation such as bending or stretching, which can severely degrade their electrical performance. Under repeated mechanical stress, MO thin films are susceptible to cracking and delamination from the flexible substrate and other layer such as source-drain electrodes. This led to interruptions of the conductive path, leading to increased resistance, device failure, and loss of functionality. Additionally, mechanical deformation induces strain-induced defects and dislocations in the MO layer. These defects act as trap sites for charge carriers, reducing mobility and causing instability in the electrical properties of the devices[33,61,101,102].

Dielectric materials are crucial for isolating different components within the TFT and enabling proper gate modulation. High-k dielectric materials, such as aluminum oxide (Al_2O_3), zirconium oxide (ZrO_2), and hafnium oxide (HfO_2), are preferred due to their high dielectric constants, which enhance capacitance and reduce operating voltage. These materials must also be deposited with low-temperature processing to be suitable for flexible substrates. Polymers and copolymers are also used for their flexibility and high dielectric constraints[103-106].

Each of these components must be carefully selected and engineered to ensure that the flexible TFTs can achieve high electrical performance while enduring the mechanical demands of bending, stretching, and other forms of deformation. The use of these advanced materials is important in developing next-generation flexible electronic devices that are not only efficient and reliable but also versatile and robust in various applications.

MO semiconductor

Semiconductor layer for high-performance

For high-performance flexible device applications such as wearable devices and AR/VR devices, the semiconductor layer must exhibit both high electron mobility and exceptional stability. Achieving these properties is critical for the development of advanced flexible and wearable electronics, which require materials that can maintain superior electrical performance under mechanical stress. In_2O_3 is extensively researched for its applications in both conductive and semiconductive roles, owing to its high electron mobility derived from the extensive overlap of its 5s orbitals. To improve carrier transport, modulate threshold voltage, and enhance stability, In_2O_3 is doped with various secondary ions[107]. Among the innovative n-type materials for this purpose are ITZO, nitrogen-doped zinc oxide (ZnON), indium tungsten oxide (IWO), hafnium indium zinc oxide (HIZO) and lithium zinc oxide (LiZnO)[108-114]. These materials improved electrical performance and stability, which ensures consistent performance over time. Shi *et al.* exhibited the fabrication and performance of bottom gate TFTs with a channel layer of ITZO and a passivation layer of GaO_x. The resulting ITZO TFTs demonstrate remarkable electrical properties, including a high field-effect mobility exceeding 58.3 $cm^2/V{\cdot}s$, a low subthreshold gate swing of 0.087 V/decade, a threshold voltage of -0.7 V, and impressive stability [Figure 2A][115]. The Sn ion contributes to the carrier path in MO, similar to the In ion in the a-ITZO channel layer, due to the similarity in the 5s orbital structures of Sn and In. Consequently, the higher content of In and Sn in the ITZO film promotes the effective intercalation of the Sn or In 5s orbitals, or increases the percolation conductivity resulting in the high mobility observed in the a-ITZO TFTs[116,117]. Recently, Li *et al.* demonstrated high-performance ITZO TFT employing water vapor during the sputtering process. These devices exhibited a high field-effect mobility of 122.10 $cm^2/V{\cdot}s$, a low threshold voltage of -2.30 V, and excellent stability under bias stress[118]. Similarly, Tiwari *et al.* fabricated flexible IWO TFTs with linear field effect mobility = 25.86 $cm^2{\cdot}V^{-1}{\cdot}s^{-1}$, subthreshold swing = 0.30 V/decade, and threshold voltage = -1.5 V [Figure 2B][111]. IWO was an appropriate material for flexible high-performance TFTs. The IWO thin films were deposited using radio frequency (RF) sputtering, followed by post-annealing at 270 °C. These films exhibited smooth morphology and high carrier density, resulting in excellent TFT characteristics. Additionally, the IWO TFTs demonstrated stable performance during bending tests. As shown in Figure 2C, Ok *et al.* investigate high-performance ZnON TFTs fabricated on PEN substrates[119]. Utilizing thermal photochemical reaction, the field-effect mobility of these TFTs is significantly enhanced from 60 $cm^2/V{\cdot}s$. Unusual variations in nanostructures were evident during the phase transformation and densification processes. In amorphous ZnO_xN_y, the separated Zn_3N_2 and ZnO nanocrystalline lattice was remarkably stabilized by reducing oxygen defects and by interfacial atomic rearrangement without breaking the nitrogen bonding. Photochemical reaction also improves device stability under bias and illumination stress, with electrical performance remaining stable after 10,000 bending cycles. ZnON has recently attracted significant interest due to its exceptional charge transport properties compared to conventional amorphous MOs. High electrical performance has been attributed to low electron effective mass and the difference in transport mechanisms compared to conventional amorphous MOs. The electron effective mass of ZnON (m_e^*/m_e = 0.19) is lower than that of IGZO (0.34 m_e^*) due to the presence of the Zn_3N_2 (0.10 m_e^*) structure[120-122].

The employing of multiple layers in flexible electronics offers several advantages. First, it allows for the enhancement of electronic properties, enabling the fabrication of devices with high performance. Second, multiple layers mitigate issues related to charge carrier recombination and trapping, which are common in single-material systems. By providing pathways for efficient charge carrier movement, multiple layers contribute to the stability and robustness of the device. Because of these advantages, many studies have been conducted[98,100,123,124]. Hsu *et al.* investigate multiple layers of titanium oxide (TiO_2) and IGZO TFTs to improve flexibility and electrical properties at a low fabrication temperature of 100 °C. The high bond enthalpy of Ti–O can be optimized by adjusting the number of oxygen vacancies to satisfy the necessary

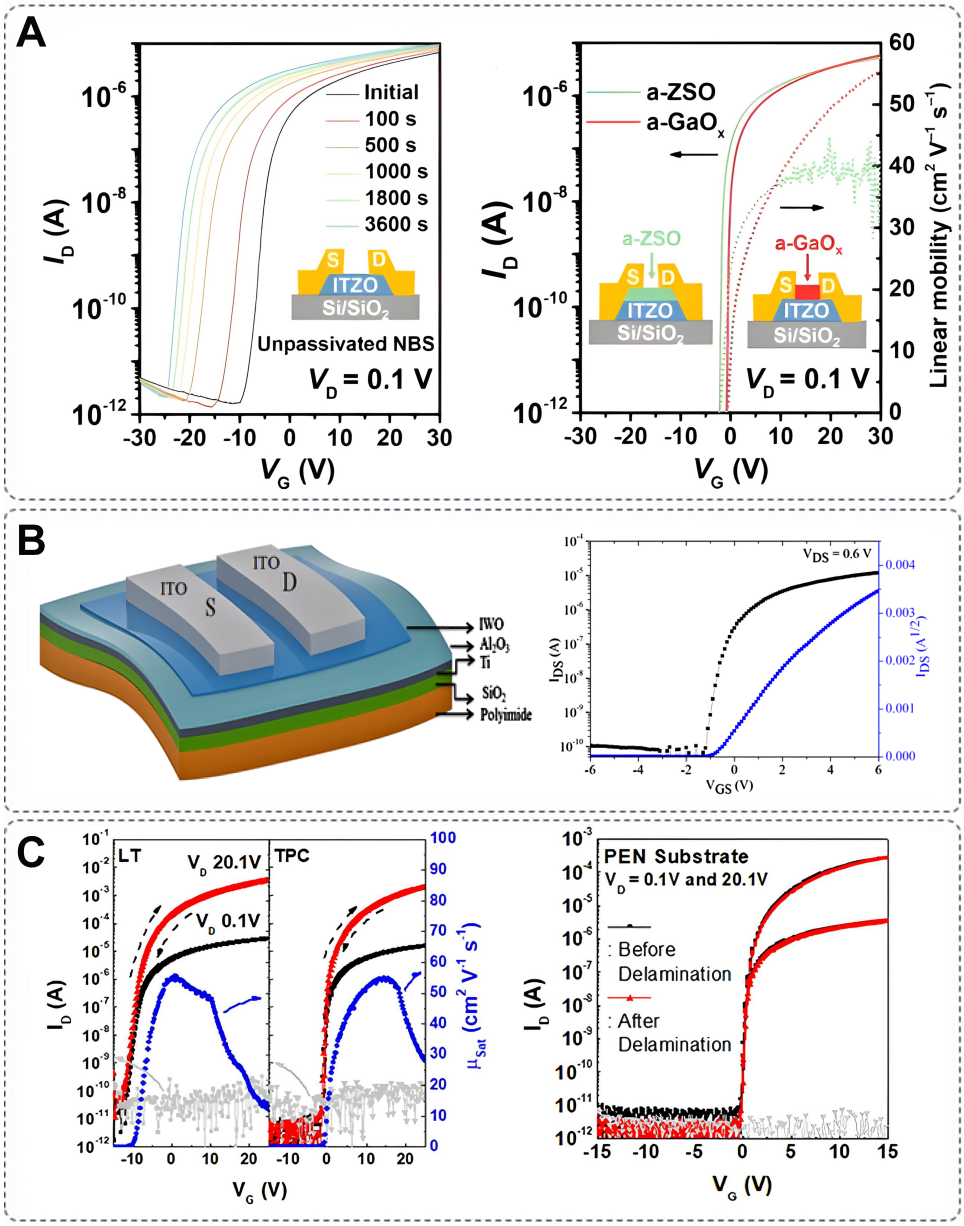

Figure 2. Electrical properties of innovative materials for high-performance flexible MO TFTs. (A) Transfer curve of ITZO TFT without the passivation under negative gate bias stress for 1 h (V_G = Vth - 20 V). Transfer curve and linear mobility of ITZO TFT with passivation by 5-nm GaO_x and ZSO. Reproduced with permission[115], Copyright 2022, AIP Publishing; (B) Schematic of fabricated flexible IWO TFTs on PI substrate and transfer characteristics IWO TFTs on SiO_2 Reproduced with permission[111], Copyright 2018, American Chemical Society; (C) Transfer characteristics of LT- and TPC-treated ZnON TFTs and saturation mobility depending on gate voltage sweep, Transfer curve of the ZnON TFTs on PEN substrate before and after delamination. Reproduced with permission[119], Copyright 2018, American Chemical Society. MO: Metal oxide; TFTs: thin-film transistors; ITZO: indium tin zinc oxide; ZSO: zinc silicon oxide; IWO: indium tungsten oxide; PI: polyimide; LT: low temperature; TPC: thermal-photochemical; PEN: polyethylene naphthalate.

specifications for gate dielectric and channel layers. The TiO_2/IGZO TFTs demonstrated superior performance with a higher field-effect mobility of 61 cm^2/V·s and a smaller subthreshold swing of 125 mV/decade at an operating voltage of 1.5 V. The devices also exhibited minimal performance degradation after bending tests, indicating excellent mechanical flexibility and stability [Figure 3A][82]. As shown in Figure 3B, Lin *et al.* introduce a novel TFT concept utilizing low-dimensional polycrystalline heterojunctions and

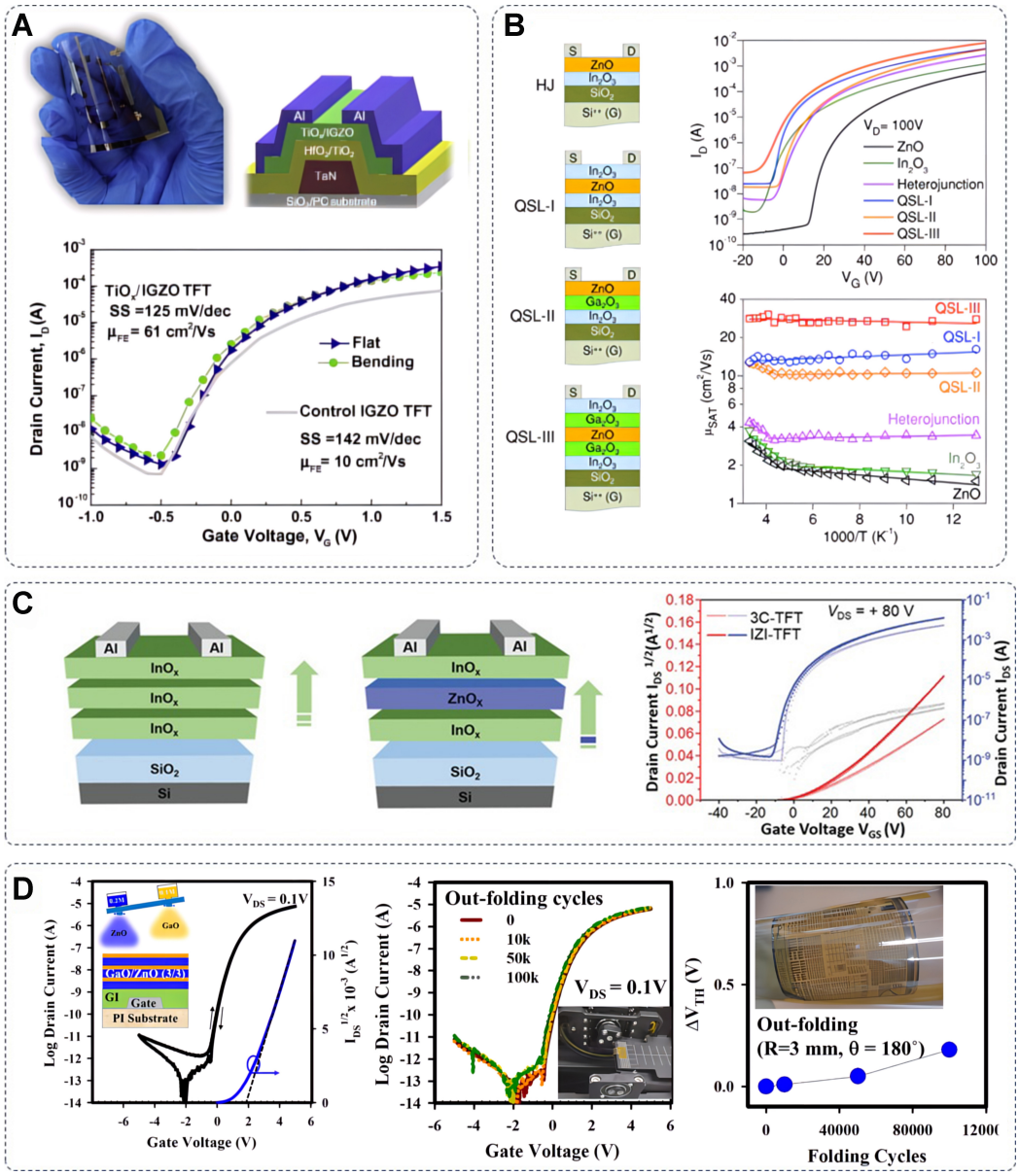

Figure 3. High-performance flexible MO TFTs employing multiple channel layers. (A) Photograph, schematic diagram, and transfer characteristics of TiO_x/IGZO TFT on PI before and after bending. Reproduced with permission[82], Copyright 2015, Elsevier; (B) Schematics of MO TFTs employing heterojunction and QSL channel layer, transfer properties of different oxide-based channel layers including ZnO and In_2O_3 and Arrhenius plots of saturation mobility depend on temperature for ZnO, In_2O_3, heterojunction, and OSLs-based TFTs measured at V_G = 80 V and V_D = 100 V. Reproduced with permission[125], Copyright 2015, Wiley-VCH; (C) Schematics and transfer characteristics of 3C-TFTs and IZI-TFTs. Reproduced with permission[99], Copyright 2022, Wiley-VCH; (D) Transfer characteristics of D4 Ga_2O_3/ZnO-stack TFTs and flexible Ga_2O_3/ZnO TFT with different folding cycles (up to 100k) and threshold voltage shift of flexible Ga_2O_3/ZnO TFT with a different folding cycle; the insets show schematic diagram for Ga_2O_3 and ZnO films on ZrO_x and the photograph of a foldable device. Reproduced with permission[98], Copyright 2022, American Chemical Society. MO: Metal oxide; TFTs: thin-film transistors; IGZO: indium gallium zinc oxide; PI: polyimide; QSL: quasi-superlattice; 3C-TFTs: triple-coated indium oxide; IZI-TFTs: indium oxide/zinc oxide/indium oxide.

quasi-superlattices (QSLs) composed of alternating layers of In_2O_3, gallium oxide (Ga_2O_3), and ZnO, created through sequential spin casting at low temperatures (180-200 °C). The optimized QSL transistors demonstrate electron mobilities of 25-45 $cm^2 \cdot V^{-1} \cdot s^{-1}$, which is about ten times higher than that of single oxide devices (2-5 $cm^2 \cdot V^{-1} \cdot s^{-1}$). The enhanced performance is attributed to quasi-2D electron gas-like systems at

the oxide heterointerfaces. This QSL transistor approach could be applied to various oxide materials and deposition techniques[125]. Recently, Tang *et al.* present an eco-friendly, streamlined method for preparing MO TFTs using a pure water-solution blade-coating process. The process focuses on low-temperature fabrication and rapid annealing process. Triple-coated indium oxide (3C-TFTs) and indium oxide/zinc oxide/indium oxide (IZI-TFTs) TFTs on SiO_2 gate dielectric (300 nm) annealed at 300 °C for just 60 s exhibit average field-effect mobility of 10.7 and 13.8 $cm^2/V{\cdot}s$, respectively. Flexible MO TFTs on PI substrates with AlO_x dielectrics exhibited a field-effect mobility of over 10 $cm^2/V{\cdot}s$ at low operating voltages. Longer annealing time of 20 min at 300 °C results in high-performance 3C-TFTs (over 18 $cm^2{\cdot}V^{-1}{\cdot}s^{-1}$) and IZI-TFTs (over 38 $cm^2{\cdot}V^{-1}{\cdot}s^{-1}$), demonstrating the effectiveness of the method for producing high-mobility, stable, and flexible TFTs [Figure 3C][99]. Bukke *et al.* fabricated the interface engineering of ZnO-based TFTs using nano-scale Ga_2O_3. By optimizing the Ga_2O_3 interface, the work achieved significant enhancements in the electrical performance and stability of the ZnO TFTs. The resulting a-Ga_2O_3/c-ZnO stack channel TFTs exhibit a high field-effect mobility of 41 $cm^2{\cdot}V^{-1}{\cdot}s^{-1}$ and excellent stability under positive bias temperature stress. On a PI substrate, a-Ga_2O_3/c-ZnO stack channel TFTs show rarely threshold voltage shifts after 100,000 bending cycles with a 3 mm radius and remain stable under environmental tests. The multiple layers of a-Ga_2O_3 and ZnO improve charge transport by enhancing heterointerfaces and reducing defect density [Figure 3D][98]. Table 1 summarized the innovative materials and multiple-layer MO for high performance.

Semiconductor layer for flexibility

To maintain electrical performance in flexible devices, the semiconductor layer must be capable of enduring mechanical stress such as bending and stretching. It is crucial that MO semiconductors endure significant physical deformation without a degradation of electrical properties. Maintaining flexibility in the semiconductor layer is therefore essential for the reliable operation of flexible devices under mechanical stress. Consequently, recent research has focused on increasing the flexibility of MO semiconductors by synthesizing other materials or forming multiple layers with other materials and MO semiconductors[128-132]. Initially, by synthesizing MOs with other materials, Liu *et al.* report on the development of high-performance transistors based on a composite of single-walled carbon nanotubes (SWNTs) and sol-gel processed indium zinc oxide (IZO). The SWNTs provide fast tracks for carrier transport, significantly enhancing the field-effect mobility to as high as 140 $cm^2/V{\cdot}s$ while maintaining a high on/off ratio of ~10^7. The composite thin films also exhibit excellent mechanical flexibility, showing superior stability with only 17% variation in performance at a bending radius of 700 μm and just 8% variation after 300 cycles of repeated bending [Figure 4A][128]. As shown in Figure 4B, Divya *et al.* proposed a new approach using water-insoluble and chemically inert polymers to form inorganic/organic composite semiconductors. These polymers resist intermixing with the oxide lattice, promote crystallization, and maintain the electrical properties of the oxide semiconductors even in near-equal amounts. As a result, optimized In_2O_3 and 25 wt% EC-based composite semiconductor TFTs exhibited linear mobility of 40-45 $cm^2/V{\cdot}s$. TFTs with high polymers endure bending tests down to a 1.5 mm bending radius without electrical performance deterioration or micro-cracks in the composite semiconductor material[129]. Na *et al.* and Kim *et al.* fabricated flexible phototransistors and flexible TFTs using organic-inorganic hybrid semiconductors based on IGZO. IGZO:PI and IGZO:PETE (polytetrafluoroethylene) TFTs fabricated by using sputter on the PI substrate. IGZO:PI phototransistors showed stable optoelectronic characteristics even after 10,000 bending tests. IGZO:PETE TFTs exhibit a field-effect mobility of 10.27 $cm^2{\cdot}V^{-1}{\cdot}s^{-1}$ and good mechanical stability with a threshold voltage shift of 0.89 V after 10,000 bending cycles at a radius of 5 mm in Figure 4C and D[130,131]. As shown in Figure 4E, Lee *et al.* form multiple layers with other materials and MO semiconductors in flexible MO TFTs. The films consist of an organic aromatic linker and indium oxide, grown using hydroquinone (HQ) as the organic precursor, bis(trimethylsilyl)amido-diethyl indium (INCA-1) as the indium precursor, and hydrogen peroxide (H_2O_2) as the oxidant. The hybrid film with semiconductor

Table 1. Summarized electrical properties and deposition method of the innovative materials and multiple-layer MO for high performance

Approach	Channel materials	Deposition method	T_{max} (°C)	μ_{FE} ($cm^2 \cdot V^{-1} \cdot s^{-1}$)	SS (V/decade)	On/off	Gate dielectric	Refs.	Year
Innovative materials	ITZO	Sputter	400	58.3	0.087	-	SiO_2	[115]	2022
	ITZO	Sputter	400	122.1	0.18	-	SiO_2	[118]	2024
	ITZO	Sputter	290	26.15	0.26	9×10^8	SiO_2	[108]	2024
	IGZTO	Sputter	400	26.8	0.15	10^8	SiO_2	[126]	2020
	IWO	Sputter	300	25.86	0.3	10^6	Al_2O_3	[111]	2018
	HIZO	Sputter	-	32.6	0.55	10^6	SiO_2	[112]	2012
	ZnON	Sputter	175	54.8	0.25	-	SiO_2	[119]	2018
	LaZnO	Spray pyrolysis	250	19.06	0.256	10^8	HfZrO	[127]	2023
	LaZnO	Spray pyrolysis	350	27.84	0.21	-	ZrO_x	[114]	2021
	LiZnO	Spray pyrolysis	350	48.47	0.256	-	ZrO_x	[114]	2021
Multiple layer	TiO_2/IGZO	Sputter	100	61	0.125	-	TIO_2/HfO_2	[82]	2015
	InO/ZnO/InO	Blade	300	38	2.8	10^6	SiO_2	[99]	2023
	(GaO/ZnO)×3	Spray pyrolysis	350	41	0.209	10^8	ZrO_x	[98]	2022
	ITO/IGZO	Sputter	300	58.2	0.12	10^{10}	AlO_x	[123]	2023
	ITZO/IGZO	Spin coater	450	51	0.41	10^8	AlO_x	[100]	2018
	InO/GaO/ZnO/GaO/InO	Spin coater	200	37	0.16	10^4	AlO_x/ZrO_2	[125]	2015

MO: Metal oxide; SS: subthreshold swing; ITZO: indium tin zinc oxide; IGZTO: indium gallium zinc tin oxide; IWO: indium tungsten oxide; HIZO: hafnium indium zinc oxide; IGZO: indium gallium zinc oxide; ITO: indium-tin-oxide.

properties is obtained at a growth temperature of 150 °C. The hybrid film with a 99:1 cycle ratio of indium oxide:indicone exhibited suitable electrical properties, including a field-effect mobility of 2.05 $cm^2/V \cdot s$, a subthreshold swing of 0.53 V/decade, a threshold voltage of 2.22 V, and excellent mechanical stability. The electrical performance remains stable even after more than 200,000 repeated bending tests with a 2 mm bending radius[132]. Table 2 summarized MO and other material compound properties for flexibility.

High-k gate dielectric

In TFTs, the gate dielectric layer is a key component that significantly influences the overall performance, energy efficiency and stability of devices during operation. As device dimensions decrease and demands for flexibility rapidly increase, traditional silicon-based dielectrics such as SiO_2 are encountering physical and electrical limitations. However, reducing the thickness of the dielectric layer to increase capacitance per unit area significantly degrades the transistor's performance and reliability because of higher leakage currents. By employing high-k dielectrics, it becomes feasible to attain higher capacitance while using thicker dielectric layers[104,105,133]. The role of high-k dielectrics in MO TFTs is to enhance the capacitive coupling between the gate electrode and the semiconductor layer. This enhancement leads to better control of the channel charge at lower gate voltage, thereby reducing power consumption and improving the switching speed of the transistor[104,105,133]. It is possible to improve the mechanical robustness of the transistor - an important property for flexible devices that are susceptible to physical stress and deformation - by using a thicker dielectric while retaining the same capacitance. Furthermore, high-k materials often demonstrate superior thermal and chemical stability compared to their low-k counterparts. This stability ensures consistent performance throughout the device lifetime, particularly under the thermal cycling and environmental stresses encountered in flexible device applications[103-105].

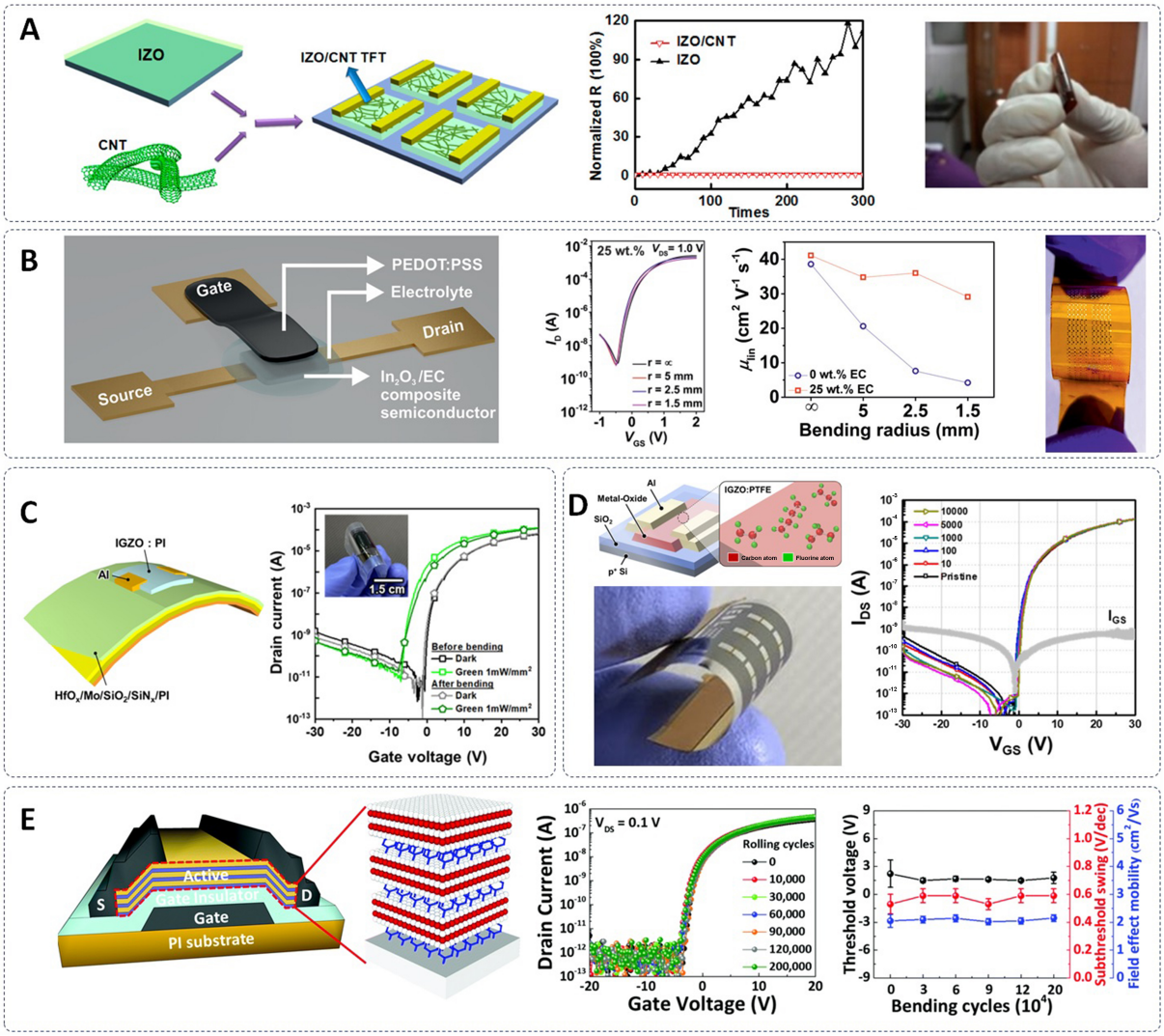

Figure 4. High-performance flexible MO TFTs with flexible semiconductors. (A) Schematic of combination IZO and CNT to fabricate IZO/CNT hybrid TFTs, the normalized resistance as a function of the folded times and the photograph that repeated bending performance of IZO/CNT hybrid TFTs. Reproduced with permission[128]. Copyright 2012, American Chemical Society; (B) Schematic of the printed InO_x/EC TFT with top-gate structure, optical image of optimized InO_x/EC TFTs on PI substrate, transfer characteristics of optimized InO_x/EC TFTs with decreasing bending radius and Change of linear mobility of optimized InO_x/EC TFTs under bending tests. Reproduced with permission[129]. Copyright 2023, Wiley-VCH; (C) Schematic of IGZO:PI phototransistor fabricated on PI substrate and Transfer characteristics before and after 10,000 bending tests under dark conditions and green light at 1 mW/mm^2 intensity. The inset shows the photograph of the bent IGZO:PI phototransistor. Reproduced with permission[130]. Copyright 2022, American Chemical Society; (D) Schematic of IGZO:PETE TFTs on SiO_2, transfer curve of the IGZO:20 W PTFE TFT in 10,000 bending cycles with bending radius of 5 mm, and photograph of IGZO:PTFE on PI substrate. Reproduced with permission[131]. Copyright 2018, American Chemical Society; (E) Schematic of device structure, transfer characteristics, and variations in electrical parameters after repeated bending 200,000 cycles of InO_x:indicone hybrid layers TFTs. Reproduced with permission[132]. Copyright 2021, Royal Society of Chemistry. MO: Metal oxide; TFTs: thin-film transistors; IZO: indium zinc oxide; CNT: carbon nanotube; EC: ethyl cellulose; PI: polyimide; IGZO: indium gallium zinc oxide; PTFE: polytetrafluoroethylene.

High-k dielectrics of MO

High-k dielectrics based on MOs exhibit excellent thermal and chemical stability compared to those based on polymers. High-performance characteristics have been investigated by several groups using high-k dielectrics of MOs, such as Al_2O_3, titanium dioxide (TiO_2), hafnium dioxide (HfO_2), yttrium oxide (Y_2O_3), and zirconium dioxide (ZrO_2), in flexible MO TFTs. Their approach to using high-k dielectrics of MO can

Table 2. Summarized compound MO single-layer and multi-stack layer properties for flexibility

Type of layer	Channel materials	Substrate	T_{max} (°C)	Bending radius (mm)	μ_{FE} ($cm^2 \cdot V^{-1} \cdot s^{-1}$)	Gate dielectric	Refs.	Year
Compound single layer	IZO/SWNT	-	350	2	63.4	SiN_x	[128]	2012
	InO/EC	-	275	1.5	40	Electrolyte	[129]	2023
	IGZO:PI	SiN_x/SiO_2	300	10	-	HfO_x	[130]	2022
	IGZO:PETE	-	380	3	3.5	SiN_x/SiO_2	[131]	2018
Multi-stack layer	InO/indicone	AlO_x	200	2	2.05	AlO_x	[132]	2021

MO: Metal oxide; IZO: indium zinc oxide; SWNT: single-walled carbon nanotube; EC: ethyl cellulose; IGZO: indium gallium zinc oxide; PI: polyimide.

be classified into three types: monolayer[72,113,114,134-137], multilayer[82,98,138-140], and doping process[141-146]. Rim *et al.* demonstrated IGZO TFTs with Al_2O_3 dielectrics on PI substrates using the direct light pattern (DLP) process, achieving patterning sizes down to a minimum feature size of 3 μm for conductors, semiconductors, and dielectrics[72]. In Figure 5A, these dielectrics exhibited a high breakdown voltage and good capacitance of ~4.9 MV·cm^{-1} and 46.3 nF at 1 kHz. The study is notable that the TFTs on PI substrates showed good performance with a high mobility of ~84.4 $cm^2 \cdot V^{-1} \cdot s^{-1}$ and an on/off ratio of greater than 10^5 at V_{DS} 1.0 V. Hsu *et al.* reported on flexible TiO_x/IGZO TFTs with bilayer HfO_2/TiO_2 dielectrics on PC substrates[82]. The bilayer structure of gate dielectrics enables maintaining a high dielectric constant while preventing gate leakage. The bottom layer of HfO_2 in the bilayer mitigates the gate leakage issue caused by a narrow ~3.3 eV bandgap of TiO_2, owing to its high bandgap. Additionally, the top layer of TiO_2, with a very high dielectric constant (> 40), efficiently accumulates charges in the channel layer. In Figure 5B, the TFTs demonstrated a high field-effect mobility of 61 $cm^2 \cdot V^{-1} \cdot s^{-1}$, a low subthreshold swing of 125 mV/decade, a low operating voltage of 1.5 V, and less property degradation after bending test. The study showed the advantages of a bilayer dielectric structure in addressing the limitations of narrow bandgap in high-k materials.

Another method of using high-k dielectrics is doping process, as demonstrated by Yang *et al.*[141]. They fabricated IZO TFTs with soluble Zr-doped AlO_x gate dielectrics on PI substrates and conducted a comparative analysis of the quantitative dielectric properties of the Zr-doped AlO_x and the undoped AlO_x films. In Figure 5C, Zr-doped AlO_x films showed lower leakage current density as the annealing temperature decreased, compared to undoped AlO_x films. Additionally, Table 3 exhibited the calculated dielectric constant of Zr-doped AlO_x (8.4-11.8) and undoped AlO_x (5.6-6.2). Doping AlO_x, which has a high breakdown field, with Zr, known for its strong bonding to oxygen, resulted in an unprecedented soluble high-k dielectric, significantly reducing the processing temperature to 250 °C. Annealing temperature, capacitance, thickness, and dielectric constant by calculation between AlO_x and Zr-doped AlO_x were compared in Table 3. This report emphasizes the feasibility of flexible IZO TFTs. The Zr-doped TFTs on ITO/PI substrates showed a saturation mobility of 51 $cm^2 \cdot V^{-1} \cdot s^{-1}$, a threshold voltage of 1.2 V, and an on/off current ratio of ~10^4.

High-k dielectrics of polymer

High-k polymer dielectrics are increasingly used in flexible and stretchable electronics due to their inherent flexibility and simple processing. Several groups have demonstrated high-performance flexible TFTs on various high-k polymer dielectrics[147-149]. Zhu *et al.* fabricated electrolyte-gated synaptic In_2O_3 TFTs on a PI substrate with polyethylene oxide (PEO) + $LiClO_4$ dissolved in acetonitrile to form the polymer electrolyte solution as gate dielectric and reported good performance electrical characteristics, exhibiting a mobility of 7.80 $cm^2 \cdot V^{-1} \cdot s^{-1}$, an on/off current ratio of ~10^6, and a threshold voltage of 0.55 V. As shown in Figure 5D, an

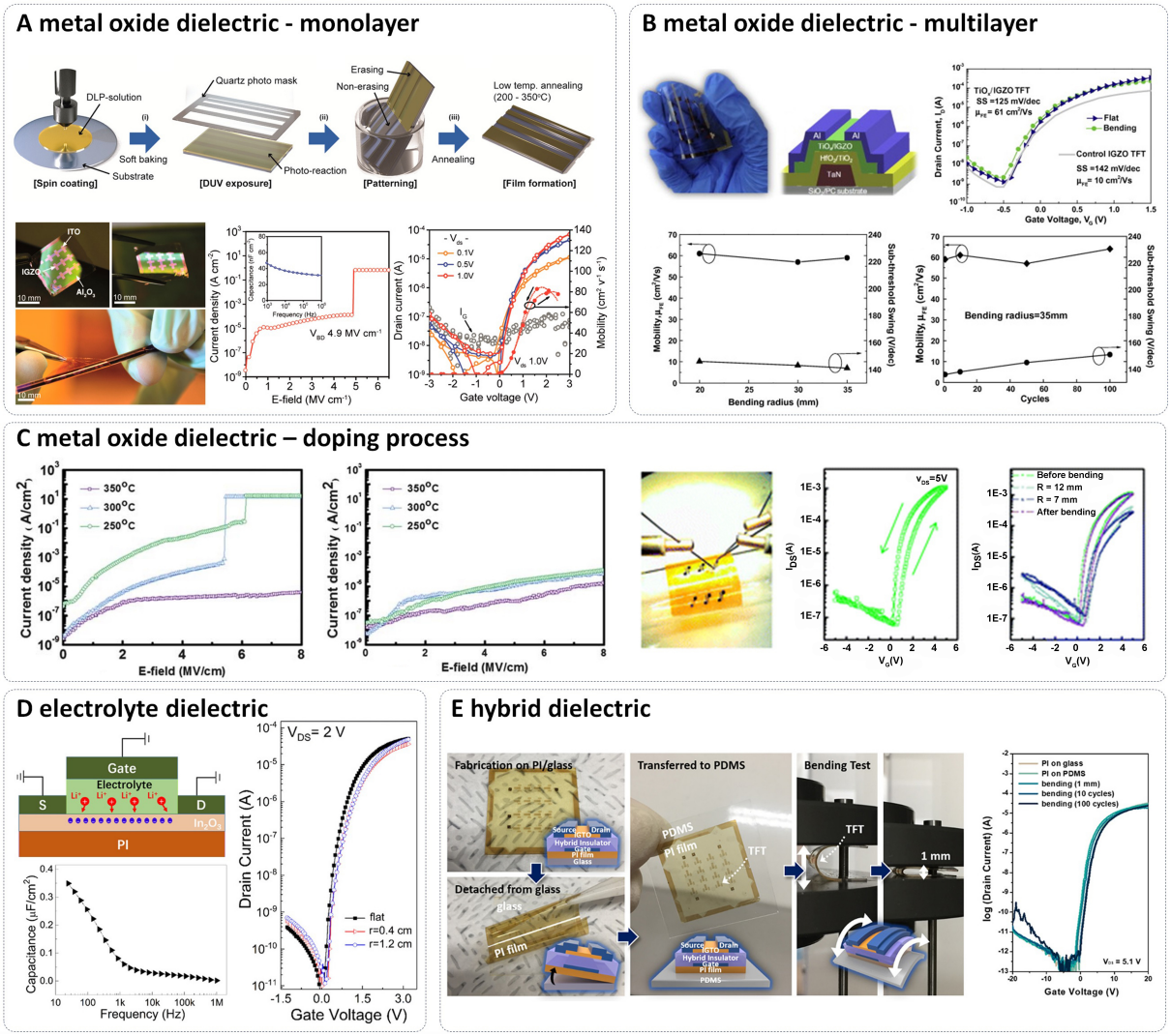

Figure 5. (A) Schematic of DLP process and film formation (top) and photographs of integrated TFTs, I-V/C-F measurement of MIM structure, and I_D-V_G curves of IGZO TFTs (bottom). Reproduced with permission[72], Copyright 2014, American Chemical Society; (B) Photograph of TFTs on PC substrate and transfer curves of TFTs (top) and electrical characteristics of TFTs under different bending conditions or cycles (bottom). Reproduced with permission[82], Copyright 2014, Elsevier; (C) Leakage current density-electric field of AlO_x and ZAO dielectric, OM image of ZAO-based TFTs on ITO/PI substrate and transfer curves of TFTs with ZAO dielectric before and after bending test. Reproduced with permission[141], Copyright 2013, The Royal Society of Chemistry; (D) Schematic of synaptic In_2O_3 TFTs, Capacitance as a function of frequency for polymer electrolyte and transfer curve of synaptic In_2O_3 TFTs on PI substrate at different bending radii. Reproduced with permission[147], Copyright 2020, American Chemical Society; (E) Photographs of integrated TFTs with bending test method and transfer curves of TFTs under different bending cycles. Reproduced with permission[149], Copyright 2019, American Chemical Society. DLP: Direct light pattern; TFTs: thin-film transistors; MIM: metal-insulator-metal; IGZO: indium gallium zinc oxide; PC: polycarbonate; ZAO: zirconium doped aluminum oxide; OM: optical microscopy; ITO: indium-tin-oxide; PI: polyimide.

electric double layer (EDL) forms at the interface between the semiconductor and the polymer electrolyte, resulting in high gate capacitance of ~0.36 μF/cm^2 and low gate voltage operations[147]. Additionally, Samanta *et al.* fabricated a-IGZO flexible TFTs on a PI Kapton substrate with an electrolyte dielectric (PEO + $LiClO_4$) and reported high-performance electrical characteristics, exhibiting a mobility of ~42 cm^2·V^{-1}·s^{-1}, an on/off current ratio of ~10^5, a threshold voltage of 0.7 V, and a low subthreshold swing of 175 mV/dec[148]. Also, these devices also form EDL, resulting in a very high gate capacitance of ~30 μF/cm^2. The study showed the stable performance of TFTs after bending test, emphasizing their valuable

Table 3. Comparison of annealing temperature, capacitance, thickness, and dielectric constant by calculation between AlO_x and Zr-doped AlO_x

Sample	T_a (°C)	Capacitance at 1 MHz (nF·cm^{-2})	Thickness	Dielectric constant
AlO_x	250	71	70	5.6
	300	84	64	6.1
	350	91	61	6.2
Zr-doped AlO_x	250	70	106	8.4
	300	90	100	10.2
	350	110	95	11.8

This table is cited with permission from Yang *et al.*, published in 2013[141], The Royal Society of Chemistry.

contributions to flexible displays. Hur *et al.* investigated IGTO TFTs on PI/PMDS film with poly(4-vinylphenol-co-methyl methacrylate) (PVP-co-PMMA)-based hybrid gate dielectrics[149]. The study improved insulating properties by reducing the residual hydroxyl groups through the incorporation of HfO_x, which has high ionicity, and accompanying ultraviolet (UV) treatment. They conducted bending test of flexible IGTO TFTs with stretchable polymer dielectrics under a bending radius (1 mm). In Figure 5E, after 100 bending cycles, TFTs exhibited good switching capability. The electrical properties of IGTO TFTs showed a field-effect mobility of 25.9 $cm^2 \cdot V^{-1} \cdot s^{-1}$, a subthreshold swing of 0.4 V/decade, a threshold voltage of -0.2 V, and an on/off current ratio of > 10^7. The study emphasized that hybrid dielectrics treated with UV are promising materials for flexible and stretchable devices requiring low-temperature processing. Table 4 summarized high-performance MO TFTs with high-k dielectrics.

Each of these components - advanced MO semiconductors, high-performance semiconductor layers, and high-k dielectrics - must be carefully selected and engineered to ensure that flexible TFTs can achieve high electrical performance while enduring the mechanical demands of bending, stretching, and other forms of deformation. The use of these advanced materials is crucial in developing next-generation flexible electronic devices that are not only efficient and reliable but also versatile and robust in various applications.

FABRICATION PROCESS FOR HIGH-PERFORMANCE MO TFT

The fabrication of high-performance flexible MO TFTs employs standard semiconductor fabrication tools to ensure precise dimensions and consistent performance. However, the diversity of flexible substrates, each with unique physical and chemical properties, requires the development of innovative techniques. Vacuum-based techniques, such as sputtering, atomic layer deposition (ALD), and pulsed laser deposition (PLD), are commonly employed for substrate deposition. Additionally, solution coating-based methods, such as spin coating, spray coating and inkjet printing, are used to create thin films for the active layers, gate dielectrics, and protective coatings. These methods are chosen for their ability to deposit uniform, dense films at low temperatures, making them compatible with flexible substrates[8,15,95]. Achieving high-performance flexible MO TFTs involves several critical steps in the fabrication process, with doping techniques playing an important role. Doping process is essential and simple for enhancing the electrical properties of MO semiconductors, improving carrier concentration, enhancing electrical stability and modulating the threshold voltage[55,95].

Doping process

Previously, several studies have attempted to improve the electrical performance of MO TFTs by doping process, such as hydrogen doping[59,151-157], nitrogen doping[110,113,157-161], fluorine doping[162-168] and metal cation doping[55-57,60]. Hydrogen doping is one of the most common techniques to improve the electrical

Table 4. Summarized high-performance MO TFTs with high-k dielectrics

Approach	Gate dielectric	Deposition method	Channel materials	Substrate	T_{max} (°C)	μ_{FE} ($cm^2 \cdot V^{-1} \cdot s^{-1}$)	SS (V/decade)	On/off ratio	Refs.	Year
MO dielectric - monolayer	Al_2O_3	Spin coating	IGZO	PI	350	84.4	-	10^5	[72]	2014
		ALD	IZO	PI	200	42.1	0.29	10^9	[134]	2016
		ALD	ZnO	PET	100	37.1	0.38	10^7	[135]	2019
		ALD	IGZO	PI	350	47.9	0.18	-	[136]	2019
		ALD	ZnON	PEN	150	147	0.21	-	[113]	2020
	HfO_2	ALD	IGZO	PI	200	19	0.09	10^{11}	[150]	2020
	ZrO_x	Spin coating	LiZnO	PI	350	48.47	0.26	10^7	[114]	2021
MO dielectric - multilayer	Ga_2O_3/ZrO_x	Spin coating	ZnO	PI	350	41	0.22	10^8	[98]	2022
	$Y_2O_3/TiO_2/Y_2O_3$	Electron beam evaporation	IGZO	PC	-	40	0.16	10^5	[138]	2013
	$SiO_2/TiO_2/SiO_2$	Electron beam evaporation	IGZO	PC	RT	76	0.13	10^5	[139]	2013
	HfO_2/TiO_2	Evaporator	TiO_x/IGZO	PC	100	61	0.13	-	[82]	2014
	Zr-Al_2O_3	Spin coating	IZO	PI	280	51	-	10^4	[141]	2013
	Al_2O_3:Nd	Anodization process	ZrInO	PEN	150	22.6	0.39	10^7	[142]	2016
Polymer dielectric	Electrolyte	Drop casting	In_2O_3	PI	250	8.74		10^6	[147]	2020
	Electrolyte	Drop casting, spin coating	IGZO	PI	120	42	0.18	10^6	[148]	2018
	PVP-co-PMMA:HfO_x	Spin cast	IGTO	PI/PDMS	150	25.9	0.4	10^7	[149]	2019

MO: Metal oxide; TFTs: thin-film transistors; SS: subthreshold swing; ALD: atomic layer deposition; IGZO: indium gallium zinc oxide; PI: polyimide; IZO: indium zinc oxide; PET: polyethylene terephthalate; PEN: polyethylene naphthalate; PC: polycarbonate; RT: room temperature; PVP-co-PMMA: poly(4-vinylphenol-co-methyl methacrylate); IGTO: indium gallium tin oxide; PDMS: polydimethylsiloxane.

performance of MO semiconductors. Incorporating hydrogen atoms into the oxide lattice can passivate defects and increase carrier mobility[59,152,153,155-157]. This process is typically done through thin film deposition in hydrogen atmosphere[152,156], hydrogen plasma treatment[153,155] or MO thin film in a hydrogen atmosphere[59,151,154]. Recently, Lee *et al.* investigated the diffusion of hydrogen from plasma-enhanced ALD (PEALD)-derived SiO_2 into the underlying a-IGZTO film during the post-deposition annealing (PDA) process. The transfer curves of the TFTs that optimized IGZTO thin films are shown in Figure 6A. Compared with those without PDA (field-effect mobility = 19.1 cm^2/Vs), the devices conducting PDA process exhibited a higher field-effect mobility of 85.9 cm^2/Vs in Figure 6A[59]. The hydrogen atoms help reduce trap states, can act as a shallow donor in MO semiconductors, and improve the overall conductivity of the semiconductor layer, leading to enhanced device performance with higher mobility and lower subthreshold swing[169,170]. However, since hydrogen doping can cause a significant negative shift in the threshold voltage (V_{TH}) and undesirable photo-instability[171,172], Abliz *et al.* demonstrated the effects of co-plasma treatment with hydrogen and nitrogen on IGZO TFTs to enhance both electrical performance and stability simultaneously[157].

Fluorine doping is a technique used to improve the stability and electrical performance of MO semiconductors. Fluorine atoms, due to their high electronegativity, can effectively passivate defect sites and reduce the density of oxygen vacancies. This leads to a decrease in off-state leakage current and an improvement in threshold voltage stability. The amount of F in MO films was carefully controlled and introduced to ZnO[163], ZTO[164,166], IGZO[167,168], InO_x[173] and IWZO[165] films to enhance electrical properties, achieving a field-effect mobility of 31.59 cm^2/Vs in ZnO TFTs[163]. Recently, Li *et al.* developed high-

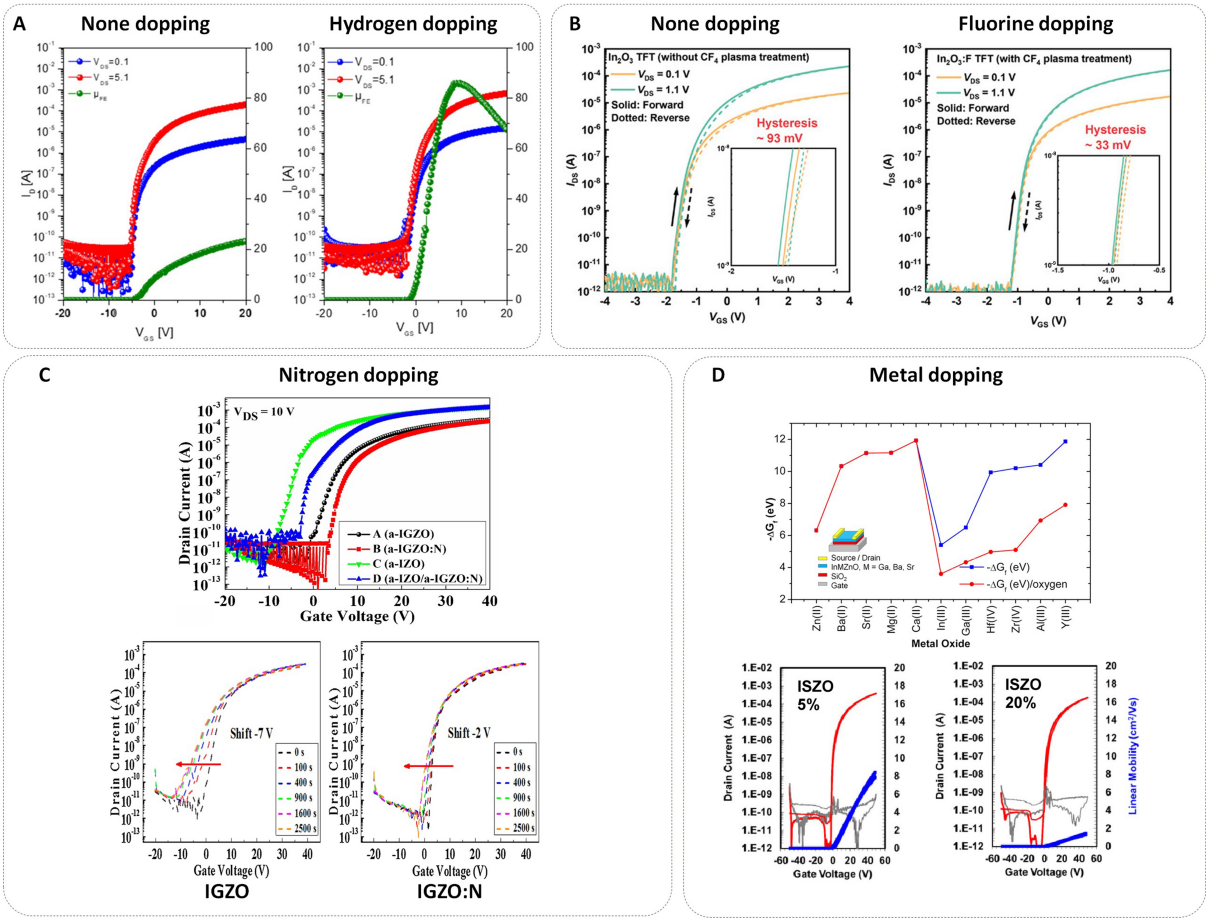

Figure 6. Doping process for the high electrical performance of MO TFTs. (A) Transfer properties of the non-passivated optimized IGZTO TFTs and SiO_2-passivated optimized IGZTO TFTs at PDA 400 °C. Reproduced with permission[59]. Copyright 2022, American Chemical Society; (B) Transfer characteristics of In_2O_3:F TFTs. Reproduced with permission[173]. Copyright 2024, Wiley-VCH; (C) Transfer characteristics of AOS TFTs, IGZO NBIS testing results and IGZO:N NBIS testing results. The stress conditions are V_{GS} = -20 V, UV light wavelength = 380 nm and UV light power = 0.1 mW/cm^2. Reproduced with permission[159]. Copyright 2016, Elsevier; (D) Gibbs Energy of oxidation calculated for metals and transfer characteristics of ISZO TFTs with different doped metal ratios. Reproduced with permission[60]. Copyright 2013, American Chemical Society. MO: Metal oxide; TFTs: thin-film transistors; IGZTO: indium gallium zinc tin oxide; PDA: post-deposition annealing; ALD: atomic layer deposition; AOS: amorphous oxide semiconductor; IGZO: indium gallium zinc oxide; NBIS: negative bias illumination stress; UV: ultraviolet; ISZO: indium strontium zinc oxide.

performance fluorine-doped indium oxide (In_2O_3:F) TFTs with enhanced bias-stress stability. This fabrication involves an ALD process using cyclopentadienyl indium (InCp) and O_2 plasma to produce a crystalline ultrathin In_2O_3 layer. Following that, a fluorine doping process using CF_4 plasma forms the In_2O_3 :F layer. Density functional theory (DFT) analysis indicated that fluorine doping stabilizes lattice oxygen and electrically passivates oxygen vacancy defects in In_2O_3 by forming F_OF_i defects. Consequently, In_2O_3:F TFTs exhibit exceptional electrical performance and bias-stress stability, achieving a high electron mobility of 35.9 cm^2/V·s, a steep subthreshold swing of 94.3 mV/dec, a minimal hysteresis of 33 mV, and a small threshold voltage shift of -111 and 49 mV under negative and positive bias stress, respectively [Figure 6B][173].

Nitrogen doping involves incorporating nitrogen atoms into the MO semiconductor to improve stability and electrical performance. Nitrogen atoms can replace oxygen vacancies in the lattice, which helps reduce the density of electron traps and improve the stability of the TFT under bias stress. Nitrogen can act both as

an acceptor and as a defect binder due to its ionic radius being similar to that of oxygen. This similarity allows nitrogen to effectively substitute for O (NO) and reduce oxygen vacancy in ZnO-based thin films[161,174]. Consequently, nitrogen doping process can enhance the bias stability of a-IGZO TFTs[158,175]. However, this process has also been associated with a decrease of mobility and a reduction of the optical band gap energy in nitrogen-doped a-IGZO TFTs[158]. Additionally, Xie *et al.* introduce nitrogen-doped AOS TFTs with a double-stacked channel layer structure combined with amorphous InZnO (a-IZO) and nitrogen-doped a-IGZO films. This TFT with a double-stacked channel layer exhibits superior field-effect mobility (up to 49.6 $cm^2/V{\cdot}s$) and stability under both bias and light stress tests compared to conventional single-layer TFTs. The enhanced performance is primarily due to the heterojunction within the channel layers and the lower interface and bulk trap densities achieved through nitrogen doping, which effectively reduces oxygen vacancies and trap sites in the channel. Additionally, the a-IGZO layer functions as a passivation layer, shielding the channel from ambient gases and UV light, further improving device stability as shown in Figure 6C[159]. Han *et al.* investigated the impact of nitrogen and IZO composition on electrical performance and stability in IZO TFTs[176]. Park *et al.* investigated nitrogen-doped ZnON TFTs on PEN substrates by employing dual gates for high performance. The effects of applying a dual gate structure are attributed to the formation of a high electron density channel away from the gate dielectric/semiconductor interface (field-effect mobility = 65.8 to 147 $cm^2{\cdot}V^{-1}{\cdot}s^{-1}$)[113].

The metal cation doping process is also widely used, and extensive research has been conducted on indium-based materials. In_2O_3 is a widely studied material for both conductive and semiconductive applications due to its high electron mobility, which results from the extensive overlap of 5s orbitals. To enhance carrier transport, In_2O_3 is typically doped with secondary ions. Sn-doped In_2O_3 (ITO) is commonly used as a transparent conductor because the difference in oxidation states between In^{3+} and Sn^{4+} leads to high carrier concentrations[95]. When doped with Ga and/or Zn (forming materials such as IGO, IZO, and IGZO), In_2O_3 achieves better semiconductor properties. Pure In_2O_3 TFTs often have high carrier concentrations, making it difficult to control off-current and V_{TH}, but Ga and Zn help mitigate this by acting as a carrier suppressor and stabilizing the amorphous state, respectively[97,177]. Other dopants are also used to enhance or stabilize the electrical characteristics of oxide semiconductors. Important factors in choosing dopants include energy bandgap, standard electrode potential (SEP), Gibbs Energy of oxidation, and electronegativity[55,60,95]. Larger bandgaps shift donor states to deeper levels, lower SEP enhances carrier suppression, and higher differences in electronegativity and Gibbs Energy of oxidation reduce V_O. Metals such as lanthanum (La), magnesium (Mg), yttrium (Y), hafnium (Hf), strontium (Sr), and barium (Ba) are effective carrier suppressors due to these properties [Figure 6D][55-57,60]. Here, electrical properties of the hydrogen, nitrogen, fluorine and other metal-doped MO semiconductors are summarized in Table 5.

Deposition method

The fabrication of high-performance flexible MO TFTs employs various deposition techniques to ensure precise dimensions and consistent performance. These methods are chosen for their ability to produce uniform, dense films at low temperatures compatible with flexible substrates. Deposition methods include sputtering, ALD, PLD, spin coating, inkjet printing, and spray coating. In addition to the standard criteria for thin-film deposition on flexible substrates, there are specific requirements critical for fabrication of flexible devices. These include maintaining low deposition temperatures compatible with the thermal limits of the flexible substrates, ensuring sufficient adhesion of the deposited materials to substrate to prevent delamination during bending, and minimizing the strain within the deposited layers to preserve the mechanical properties, such as bendability, of the final devices[10,12,15,95].

Table 5. Summarized electrical characteristics of various materials dopped MO semiconductors

Doping materials	Channel materials	Deposition method/doping method	T_{max} (°C)	μ_{FE} ($cm^2 \cdot V^{-1} \cdot s^{-1}$)	SS (V/decade)	On/off ratio	Gate dielectric	Refs.	Year
H doping	ZnO	Sputter/UV irradiation	300	14.2	-	10^6	SiN_x	[151]	2018
	IZTO	Sputter/ESL deposit by PECVD	350	48	0.15	10^{10}	SiO_2	[154]	2015
	IGZO/IGZO:H	Sputter/H_2 plasma	250	55.3	0.18	10^8	SiO_2	[153]	2016
	IGZTO	Sputter/passivation deposit by PEALD	400	85.9	0.33	-	SiO_2	[59]	2022
	IGZO	Sputter/using sputter gas (Ar/H_2)	200	16.15	-	-	SiO_2	[156]	2018
	IGZO	Sputter/H_2 plasma	150	36.6	0.4559	-	SiO_2	[155]	2020
	ZnO	Sputter/H_2 plasma	200	12.1	2.702	-	SiO_2	[155]	2020
	In_2O_3	Sputter/H_2 plasma	RT	55.9	1.435	-	SiO_2	[155]	2020
F doping	ZnO	Spray pyrolysis/NF_3 plasma	350	31.59	0.238	10^8	ZrAlO	[163]	2021
	ZTO	Co-sputter (ZnO/FTO)	350	14.2	0.087	10^9	AlO_x:Nd	[166]	2023
	IWZO	Sputter/CF_4/N_2 + O_2 plasma	400	31.2	0.37	10^6	HfO_2	[165]	2020
	IGZO	Sputter/CHF_3/O_2 plasma	400	39.8	0.21	10^6	HfLaO	[167]	2014
	InO_x	ALD	150	35.9	0.094	-	Al_2O_3	[173]	2024
N doping	IGZO	Sputter using Ar,N_2 gas	300	19.21	0.26	-	SiO_2	[158]	2016
	IGZO:N/IZO	Sputter using Ar,N_2 gas	300	49.6	0.5	10^7	SiO_2	[159]	2016
	ZnON	Sputter using $Ar/O_2/N_2$ gas	250	51.99	0.42	10^8	SiO_2	[110]	2015
	ZnON	Sputter using $Ar/O_2/N_2$ gas	-	65.8	0.48	-	Al_2O_3	[113]	2020
	IGZO	PEALD/N_2 plasma	350	106.5	0.113	-	Al_2O_3	[161]	2023
	ZnON	ALD	250	4.8	0.47	10^7	Al_2O_3	[160]	2018
	IZO	Sputter	350	24.67	0.41	10^9	SiO_2	[176]	2016
Metal doping	IBZO	Spin coating	450	18	-	-	SiO_2	[60]	2013
	ISZO	Spin coating	450	25	-	-	SiO_2	[60]	2013
	LaZnO	Spray pyrolysis	350	27.84	0.21	-	ZrO_x	[114]	2021

MO: Metal oxide; SS: subthreshold swing; UV: ultraviolet; IZTO: indium zinc tin oxide; ESL: etch stopper layer; PECVD: plasma-enhanced chemical vapor deposition; IGZO: indium gallium zinc oxide; IGZTO: indium gallium zinc tin oxide; PEALD: plasma-enhanced atomic layer deposition; ZTO: zinc tin oxide; FTO: fluorine tin oxide; IWZO: indium tugsten zinc oxide; IZO: indium zinc oxide; ALD: atomic layer deposition; IBZO: indium barium zinc oxide; ISZO: indium strontium zinc oxide.

Sputtering is the predominant technique used to deposit vacuum-processed MO semiconductors. It involves bombarding a target material with high-energy particles, causing atoms to be ejected and deposited onto a substrate. Sputtering techniques include RF, RF-magnetron, direct current (DC), and pulsed DC sputtering. These methods have been widely used to deposit materials such as IGZO, IZO, ITZO, and ZnO[111-113,118,126,178]. The advantages of sputtering are its large availability of tools, low-temperature deposition (typically at room temperature), good adhesion, and dense structure of the final layers. Additionally, sputtering tools offer several opportunities to optimize the layer properties by adjusting the power and/or sputtering pressure. Reactive sputtering, which uses different concentrations of Argon (Ar) and O_2, can be employed to adjust the oxygen content in MO semiconducting active layers[179]. Furthermore, co-sputtering techniques using targets such as IZO and Ga_2O_3 enable better control of the stoichiometric composition of IGZO[10,12,94,179]. PLD is another effective method for depositing MOs such as IGZO, Ga_2O_3 and ZITO[92,148,180]. This technique involves using a high-power pulsed laser beam to vaporize a target material, which then deposits onto a substrate. PLD is known for producing high-quality films with excellent uniformity and stoichiometry control[181,182]. Although the process requires high temperatures, it results in high-quality thin films that are crucial for the performance of flexible TFTs. ALD is a vapor-phase technique used to deposit thin films with atomic-level precision. It involves the sequential use of gas-phase chemical processes to

deposit materials one atomic layer at a time. ALD is particularly advantageous for creating conformal coatings with excellent uniformity and control over film thickness. It has been used to deposit materials such as Al_2O_3 and HfO_2[92,111,113,123,135]. Recently, ALD and PEALD have also been used for the deposition of semiconductors such as IGZO, ZnO and InO_x[134-136]. These materials are gaining attention for their excellent electrical properties and suitability for use in advanced electronic devices, including TFTs and optoelectronic components. PEALD is a variant that uses plasma to enhance the reactivity of the precursors, allowing for lower-temperature processing. ALD and PEALD are well-suited for depositing channel layers, gate dielectrics, and passivation due to their ability to produce films with high resistance, low pinhole density, and good sidewall coverage[183].

Spin-coating is a widely used technique for fabricating oxide thin films on flexible substrates due to its simplicity, uniformity, reproducibility, and compatibility with various substrates[8,15]. The process involves depositing a liquid precursor on a substrate, which is then rapidly spun to evenly distribute the solution, balancing centrifugal and viscous forces. This results in a thin, uniform film treated by drying and annealing after spin coating. The film thickness is influenced by factors such as rotational speed, duration, and solution viscosity. Spin-coating can deposit films with a minimum thickness of around 5 nm and is suitable for solutions with viscosity between 1 and 5,200 cP[8,184,185]. Despite its advantages, spin-coating has limitations, including material wastage, difficulty with large or curved substrates, and low throughput. In contrast, methods such as slit-die coating can improve uniformity. Spray-coating is a cost-effective, noncontact method for depositing thin films over large areas using small amounts of MO solution deposition. This technique allows for material doping and multicomponent film through multiple coating processes. It uses an atomizer or nebulizer to create fine droplets from low-viscosity solutions, which are directed onto a substrate by carrier gases and gravity, with an electrostatic field aiding in the formation of thin-film coatings. The thickness, roughness, and quality of the films are influenced by droplet size, coating cycles, substrate temperature, and solution viscosity during thin-film deposition. While capable of achieving film thicknesses of 10-600 nm and handling viscosities of 0.1-1 cP[8,186], spray-coating faces challenges such as high film roughness, limited low-viscosity solutions, and lengthy processing times. Despite these issues, it remains valuable for large-area thin-film deposition due to its simplicity and adaptability. Inkjet printing, a noncontact thin-film deposition technique, is valued for its precision and efficiency. It uses micrometer-scale nozzles in printer heads, with thermal inkjet expelling ink via solvent evaporation and piezoelectric inkjet using voltage-induced nozzle shape changes. Factors including nozzle diameter, temperature, and type affect the morphology of printed patterns. Ink viscosities range from 1 to 50 cP, and printed lines are 20 to 50 μm wide[8]. While inkjet printing offers advantages involving photolithography-free deposition, selective small-area coating, and efficient material use, it faces challenges such as lower throughput compared to roller-based methods, limited ink choices, and potential nozzle clogging. Moreover, 3D printing is emerging as a promising fabrication method for flexible MO TFTs due to its ability to create complex, custom geometries with precise control. This technique enables the layer-by-layer deposition of functional materials allowing for the formation of TFTs on flexible substrates. For MO TFTs, 3D printing offers several benefits, including the precise deposition of MOs and integration with flexible substrates without the need for high-temperature processing, which is often incompatible with flexible materials. Additionally, 3D printing reduces waste and provides greater design flexibility compared to conventional methods. Recent studies have demonstrated successful printing of oxide semiconductors using inkjet or aerosol jet printing techniques, showcasing the potential of 3D printing in this area. However, challenges remain, particularly in ensuring the uniformity and electrical performance of printed MOs; nevertheless, continued advancements in 3D printing materials and techniques are making flexible MO TFT fabrication increasingly feasible[187-190].

While each technique offers distinct advantages, they also have drawbacks. PLD requires high temperatures and long processing times, while ALD has a slow deposition rate and is limited in scalability for large areas. Spin-coating suffers from material wastage and difficulties in achieving uniform coatings on large or curvature substrates. Spray-coating faces issues with high film roughness and long processing times. Inkjet printing, though precise, has lower throughput and limited ink choices due to viscosity and clogging concerns. Despite these challenges, each of these deposition methods offers unique advantages and specific applications, playing a crucial role in fabricating high-performance flexible MO TFTs and enabling the development of advanced flexible electronic devices with improved electrical properties and mechanical flexibility. Table 6 is a comprehensive overview of deposition techniques, the materials deposited, and the electrical properties of materials.

DEVICE STRUCTURE

Flexible MO TFTs affect repeated bending stress. Repeated bending stress in MO TFTs creates oxygen vacancies, generating carriers and causing a negative V_{TH} shift, increased saturation mobility, and higher drain current. This occurs because strain-induced atomic distance expansion reduces the energy band gap (ΔE) between bonding and antibonding orbitals, leading to more electrons in the antibonding state. It increases electron density in the conduction band and MO conductivity which affect V_{TH} negatively[191,192]. Strain-induced oxygen vacancies also increase electron density, further contributing to the negative V_{TH} shift. Therefore, extensive research is being conducted on structures that are less affected by mechanical stress to reduce these negative impacts. The structure of flexible MO TFTs can be varied, generally falling into three categories: island structure TFTs, junctionless TFTs, and electrode and channel layer architecture.

Island structure TFTs, as the name suggests, are fabricated on substrates featuring either an island structure or a flat substrate with islands created. In this architecture, the MO TFTs are fabricated on isolated islands in the substrate as presented in Figure 7. This structure offers several advantages, including reduced leakage current and enhanced device reliability. Island structure TFTs are commonly implemented in flexible displays, where high performance and uniformity are essential.

Junctionless TFTs are characterized by the absence of a boundary between the source-to-drain electrode and the channel layer. Unlike traditional TFTs, which form source-to-drain and channel junctions, junctionless TFTs utilize a single semiconductor material for both the channel and the electrodes. This simplifies the fabrication process and reduces manufacturing costs. In junctionless TFTs, there is no overlap region between the source/drain (S/D) and gate electrodes. Consequently, parasitic capacitances are not present, making them suitable for high-speed and low-power applications such as integrated circuits and sensors.

Flexible TFTs employing electrode and channel layer architecture release flexible stress by distributing mechanical stress within the devices. The electrode and channel layer architecture serves to distribute mechanical stress, preventing the deformation or failure of the active semiconductor layer during bending or stretching. By mitigating mechanical stress, TFTs utilizing an electrode architecture exhibit enhanced mechanical reliability and durability. Island structure TFTs offer improved performance and reliability but may require more complex fabrication processes. Junctionless TFTs simplify device fabrication and reduce costs but may exhibit lower carrier mobility compared to traditional TFTs. TFTs utilizing electrode architecture enhance mechanical reliability but may introduce additional processing steps and electrode conductivity issues depending on the electrode architecture. In this part, the configurations, examples of implementation, advantages, limitations, and potential uses of each structure of flexible MO TFTs are reviewed and discussed in detail.

Table 6. Summarized deposition techniques, the materials deposited, and the electrical properties of materials

Deposition method	Channel materials	T_{max} (°C)	μ_{FE} ($cm^2 \cdot V^{-1} \cdot s^{-1}$)	SS (V/decade)	On/off ratio	Gate dielectric	Refs.	Year
Sputter	IZTO	380	52.4	0.2	10^8	SiO_2	[178]	2014
	ITZO	400	122.1	0.18	-	SiO_2	[118]	2024
	ITZO	290	26.15	0.26	10^8	SiO_2	[108]	2024
	IGZTO	400	26.8	0.15	10^8	SiO_2	[126]	2020
	IWO	300	25.86	0.3	10^6	Al_2O_3	[111]	2018
	HIZO	-	32.6	0.55	10^6	SiO_2	[112]	2012
ALD	IZO	200	42.1	0.29	10^9	Al_2O_3	[134]	2016
	ZnO	100	37.1	0.38	10^7	Al_2O_3	[135]	2019
PEALD	IGZO	200	70	0.25	10^8	SiO_2	[136]	2019
Spray pyrolysis	LaZnO	250	19.06	0.256	10^8	HfZrO	[127]	2023
	LaZnO	350	27.84	0.21	-	ZrO_x	[114]	2021
	LiZnO	350	48.47	0.256	-	ZrO_x	[114]	2021
	(GaO/ZnO)×3	350	41	0.209	10^8	ZrO_x	[98]	2022
Spin coating	InO/GaO/ZnO/GaO/InO	200	37	0.16	10^4	AlO_x/ZrO_2	[125]	2015
	ITZO/IGZO	450	51	0.41	10^8	AlO_x	[100]	2018

SS: Subthreshold swing; IZTO: indium zinc tin oxide; ITZO: indium tin zinc oxide; IGZTO: indium gallium zinc tin oxide; IWO: indium tungsten oxide; HIZO: hafnium indium zinc oxide; ALD: atomic layer deposition; IZO: indium zinc oxide; PEALD: plasma-enhanced atomic layer deposition; IGZO: indium gallium zinc oxide.

Island structure

Flexible MO TFTs on an island-structured substrate are less affected by mechanical stress due to several reasons. The island structures help distribute mechanical stress evenly across the substrate, preventing localized stress concentrations that could damage flexible TFTs. Additionally, the islands isolate deformation to specific areas, reducing the overall strain experienced by the TFTs and limiting the impact of bending or stretching on their active regions. In 2021, Han *et al.* demonstrated IGZO TFTs initially fabricated on PI islands and then transferred onto a thermoplastic polyurethane (TPU) film. Due to a lower elastic modulus of TPU compared to PI, this configuration significantly reduced the curvature of the PI island, even under the same bending test conditions. Flexible MO TFTs with island structure and an organic passivation layer exhibited decreases in the threshold voltage by -0.22 V and the saturation mobility by -2.3% even after 250,000 repetitive bending tests. These devices, utilizing an organic passivation layer, exhibited that the NMOS pseudo inverter and NAND gate also maintained electrical performance without significant degradation in 100,000 repeated bending tests. Following repeated mechanical stresses, the high output voltage (VOH) and low output voltage (VOL) of the inverter changed minimally from 8.85 to 8.93 V and from 0.44 to 0.50 V, respectively. In NAND gates, VOH and VOL exhibited slight changes from 8.46 to 8.56 V and from 0.45 to 0.55 V, respectively [Figure 7A][102]. Kim *et al.* also developed flexible IGZO TFTs on a PI substrate using mesa island structure and photochemical activated combustion sol-gel a-IGZO. The fabricated flexible MO TFTs included a solution process AlOx as a gate dielectric layer and showed a field-effect mobility of 6.06 $cm^2 \cdot V^{-1} \cdot s^{-1}$ and a threshold voltage of -0.99 V with less than 9% variation, followed by 10,000 bending cycles with a radius of 125 μm as shown in Figure 7B. Importantly, the monolithic site-specific formation of mesa island structured devices enables the fabrication of fully integrated logic circuits such as ring oscillators which meet the industrial requirements for device density and scalability. The effect of island structure on flexible MO TFTs was analyzed under mechanical stress through mechanical simulation using finite-element analysis (FEA) method in Figure 7B. This report showed the stress profiles in a-IGZO TFTs on both planar and mesa island structures, focusing on areas near the maximum stress region. It indicated that the mesa island structure significantly reduces and redistributes the induced stress, lowering it by approximately an order of magnitude across most device regions[33]. Park *et al.* also investigate

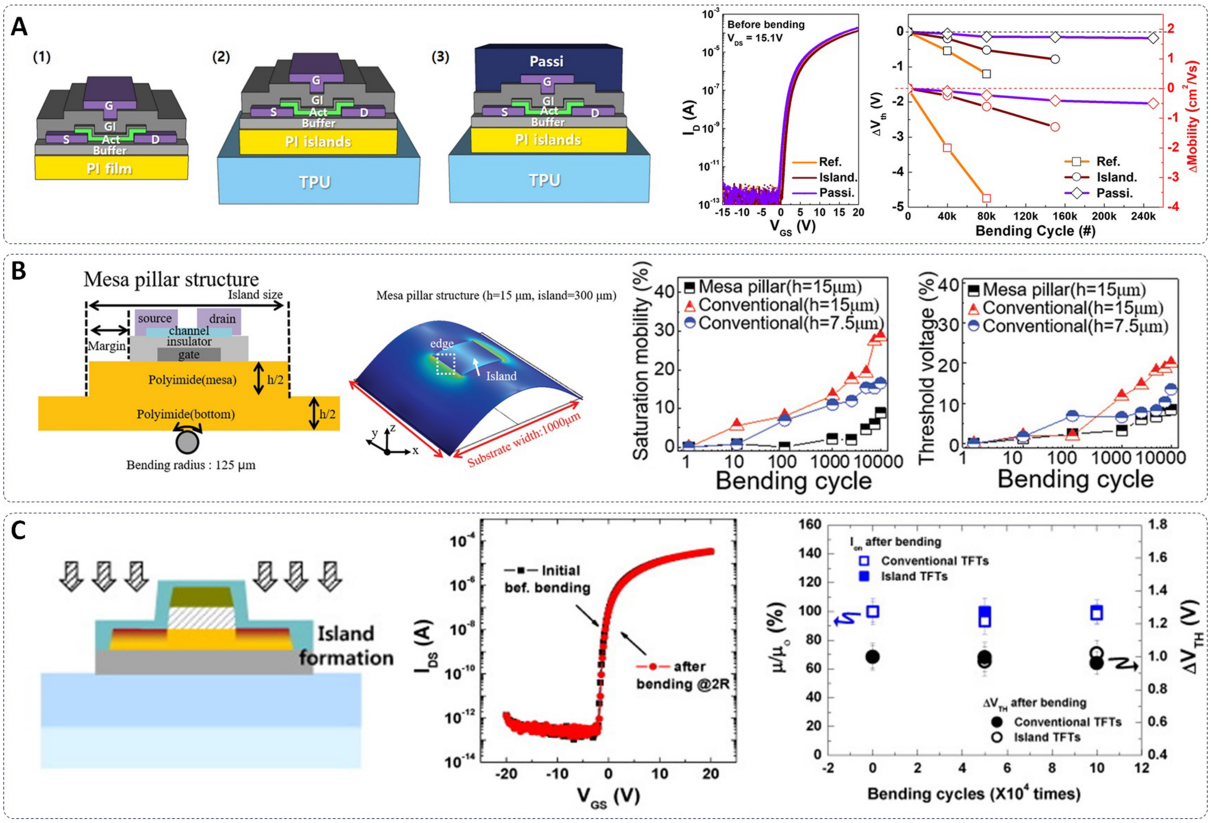

Figure 7. Flexible MO TFTs employing island structure. (A) Schematic of the three different types of top gate a-IGZO TFTs, photograph of island a-IGZO TFT with passivation. Transfer characteristics of three types of a-IGZO TFTs before the bending test. Changes in electrical properties of the TFTs repeated bending cycle. Reproduced with permission[102]. Copyright 2021, American Chemical Society; (B) Schematic of a-IGZO TFT fabricated with mesa-island structure. 3D image for mechanical stress distribution of mesa-island structure using FEA modeling to analyze mechanical stress. Normalized electrical characteristics of a-IGZO TFTs on island structure and conventional structure before and after 10,000 bending cycles under a bending radius of 125 μm. Reproduced with permission[33]. Copyright 2020, Wiley-VCH; (C) Schematic of island structure formation of a-IGZO TFTs. Transfer characteristics of the devices with island structure and the electrical responses of the devices as a function of the accumulated stress after 100,000 bending cycles at a radius of 2.0 mm. Reproduced with permission[193]. Copyright 2016, Elsevier. MO: Metal oxide; TFTs: thin-film transistors; IGZO: indium gallium zinc oxide; FEA: finite-element analysis.

the electrical performance and mechanical resilience of a-IGZO TFTs on a PI substrate under repeated bending stress. Conventional coplanar TFTs are compared with those using an island structure, both positioned at various distances from the neutral plane. A change in saturation mobility and threshold voltage of island structured a-IGZO TFTs is less than 10% in Figure 7C. The results exhibited that the island structure significantly suppresses strain-induced electrical degradation, maintaining high mechanical stability even when placed up to 50 μm from the neutral surface. It demonstrated the potential of island-structured a-IGZO TFTs in flexible electronics, such as foldable and rollable displays, by effectively distributing mechanical strain and enhancing device stability [Figure 7C][193].

However, this substrate architecture requires additional fabrication processes, leading to rising manufacturing costs compared to conventional structure MO TFTs. Simplifying the fabrication process is needed to address this issue.

Junctionless structure

The flexible TFTs can experience stress concentration at the S/D and channel junction, potentially causing deformation and delamination between the channel and the S/D electrodes which increase in contact resistance under mechanical stress[63-66,194-198]. The increase in contact resistance degrades the device. However, flexible MO TFTs employing junctionless structure have no S/D electrode and channel junction. Therefore, mechanical stress is not concentrated at the S/D electrode and channel junction under mechanical. It is also less affected by the change of contact resistance caused by mechanical stress. In 2021, Yuan *et al.* demonstrate the fabrication of junctionless EDL TFTs on paper substrates, utilizing a solution-processed chitosan dielectric [Figure 8A]. The TFTs operate at a low voltage of 1.0 V, thanks to the high gate capacitance provided by the EDL effect. The devices show excellent field-effect mobility, subthreshold swing, and current on/off ratio. The EDL effect originated by forming a layer of charged ions at the interface with an electrode in electrolyte under an electric field. This results in a high capacitance exhibited significant modulation of the electric field with low voltage [Figure 8A]. In TFTs employing ITO channel layers and S/D, the EDL effect enables low-voltage operation by effectively controlling the channel conductivity, making these devices suitable for low-power, flexible, and portable electronics[66]. This work demonstrates the potential of these junctionless EDL TFTs for flexible electronic applications such as portable sensors and smart labels. The devices are noted for their low power consumption and simple fabrication process. Additionally, Jiang *et al.* also fabricated flexible junctionless oxide-based EDL TFTs on paper substrates at room temperature. The flexible TFTs utilize ITO films for both the channel and S/D electrodes, eliminating the need for S/D junctions. These devices demonstrate effective field-effect modulation with thin ITO films. The flexible junctionless TFTs exhibited excellent device performance, including a small subthreshold swing and a large on/off ratio[64]. These characteristics suggest significant potential for flexible paper electronics and low-cost portable sensors. Dou *et al.* focus on dual-gate TFTs (DGTFTs) on paper substrates, using solution-processed chitosan-based proton conductors as the gate dielectric. The dual-gate configuration allows for precise threshold voltage modulation and logic functionality [Figure 8B]. The devices demonstrate AND logic circuits, making them suitable for various logic applications. The DGTFTs exhibit stable performance and good switching characteristics. The simple and low-cost fabrication process, along with the excellent electrical properties, makes these devices promising for flexible electronics. The study exhibited the benefits of DGTFTs in terms of threshold voltage control and logic operations, emphasizing their potential in flexible and portable electronic applications[194]. Recently, Jeon *et al.* report on the development of flexible, transparent junctionless TFTs with oxygen-plasma treatment ITO channels on PI substrates [Figure 8C]. The devices are patterned using photolithography, which simplifies the fabrication process. The TFTs exhibited stable performance even under bending conditions. This study demonstrated that the junctionless structure offers advantages for flexible devices and reliable operation under mechanical stress through mechanical simulations using FEA method [Figure 8C]. The study emphasizes the advantages of the junctionless structure for flexible devices and the simplicity of the fabrication process[198]. However, junctionless TFTs, while advantageous for their simplified fabrication, have several drawbacks. They tend to exhibit higher off-state leakage currents and larger subthreshold swings, and their performance is sensitive to fabrication variations[63-66,194-197].

However, if these issues are resolved, junctionless TFTs could become highly efficient and reliable components in flexible electronics, offering simplified fabrication and enhanced performance with low power consumption. These devices provide ease of fabrication and show great potential for applications in the field of flexible electronics.

Electrode and channel layer architecture

Flexible TFTs rely heavily on advanced electrode architectures to maintain performance under mechanical stress. The key challenge is to minimize the stress concentration at the electrode regions, which can lead to

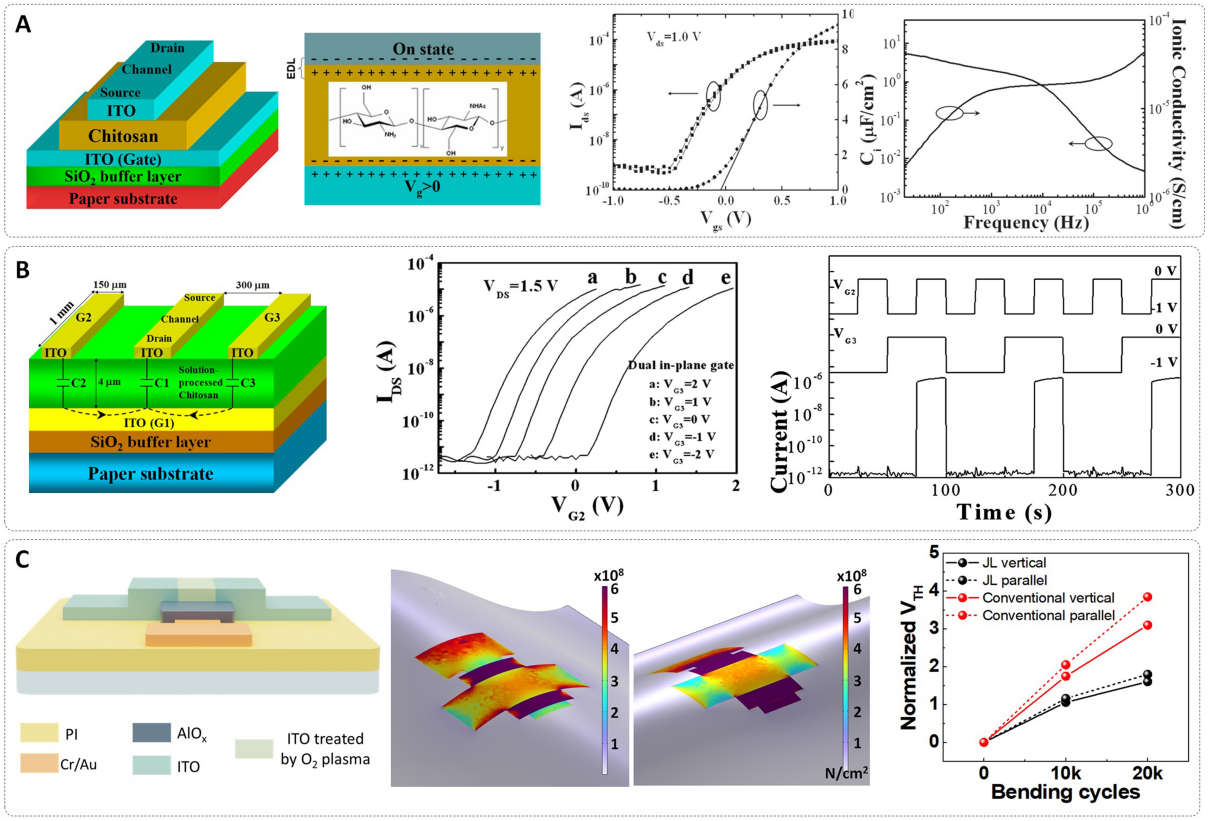

Figure 8. Flexible MO junctionless TFTs. (A) Schematic of junctionless ITO TFTs with chitosan dielectric and EDL formation. Transfer characteristics of junctionless ITO TFTs with chitosan dielectric. Dependence of capacitance and conductivity on frequency for solution-processed chitosan dielectrics. Reproduced with permission[66]. Copyright 2021, Electrochemical Society; (B) Schematic of junctionless ITO TFTs employing dual gate on paper substrate. Transfer characteristics of junctionless ITO TFTs employing dual gate on paper substrates with VG_3 ranging from 2 to -2 V. AND logic function of junctionless ITO TFTs employing dual gate. Reproduced with permission[194]. Copyright 2021, American Chemical Society; (C) Schematic of ITO junctionless TFTs on plastic substrates. Transfer characteristics of ITO junctionless TFTs before and after bending. Output characteristics of ITO junctionless TFTs on PI substrates. Reproduced with permission[198]. Copyright 2024, American Chemical Society. MO: Metal oxide; TFTs: thin-film transistors; ITO: indium-tin-oxide; EDL: electric double layer; PI: polyimide.

cracks and performance degradation. One effective approach is to use mesh and strip patterns for source/drain/gate (S/D/G) electrodes. Lee *et al.* demonstrated that a-IGZO TFTs with mesh-patterned S/D electrodes and strip-patterned semiconductor layers show no crack generation even after 60,000 bending cycles with a radius of 0.32 mm[61]. This design significantly enhances the mechanical stability of the TFTs by distributing the mechanical strain more evenly across the device. Another critical aspect of electrode architecture is the choice of materials. Metals such as molybdenum (Mo) are commonly used due to their high conductivity and good ohmic contact with the semiconductor layer. However, Mo electrodes are brittle under bending stress. To overcome this, Lee *et al.* incorporated micrometer-sized patterns to reduce crack formation. The study showed that by reducing the line width of Mo electrodes to 6 μm, no cracks were observed even after 4,000 bending cycles. This indicates that micrometer patterning of S/D/G electrodes can significantly improve the robustness of flexible TFTs [Figure 9A][61]. The active layer splitting in back-channel-etched (BCE) and etch-stopper (ES) TFTs on PI substrates offers another significant improvement in performance and stability. Lee *et al.* demonstrated that by splitting the active layer into smaller sections, the mobility of the TFTs could be enhanced significantly. The study exhibited that splitting the active layer into 2-4 μm widths along the channel led to increased saturation mobility from 24.3 to 76.8 $cm^2/V{\cdot}s$, with a subthreshold swing of less than 80 mV/dec. This improvement was attributed to the enhanced top interface

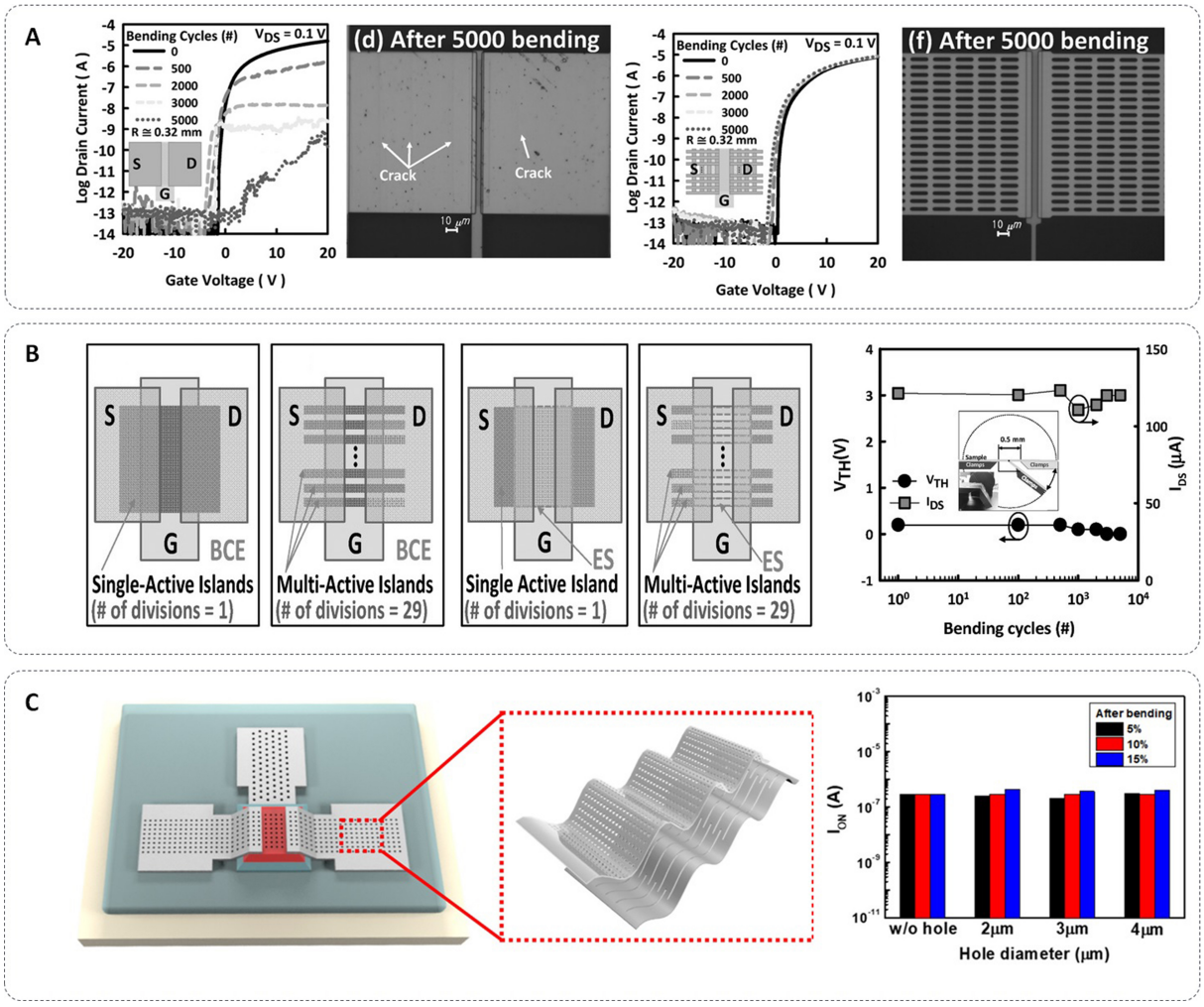

Figure 9. Flexible MO TFTs employing channel and electrode architecture for mechanical flexibility. (A) Transfer characteristics and optical images of conventional and metal mesh electrode and strip semiconductor a-IGZO TFTs after 5,000 bending cycles. Reproduced with permission[61]. Copyright 2017, Wiley-VCH; (B) Structures of BCE a-IGZO TFTs on flexible substrate with BCE and with BCE-SP, and of the etch-stopper a-IGZO TFTs with ES and ES-SP. The results of bending cycle for threshold voltage and drain current at V_G = 10 V and V_D = 20 V for the flexible IGZO TFTs employing SP with 4 μm unit width after 5,000 bending at a radius of 1 mm. Reproduced with permission[67]. Copyright 2017, Wiley-VCH; (C) Schematic of the flexible thin film transistor and electrode employing the hole structure. On current before and after bending. The results are compared according to the existence of holes, diameters, and percentages. Reproduced with permission[62]. Copyright 2017, American Chemical Society. MO: Metal oxide; TFTs: thin-film transistors; IGZO: indium gallium zinc oxide; BCE: back-channel-etched; SP: split active layers; ES: etch-stopper.

quality due to the incorporation of fluorine (F) at the interface, which reduces defect density and improves electron mobility. The split active layer structure also demonstrated excellent mechanical stability after 5,000 bending cycles at a 1 mm radius, showing minimal changes in V_{TH} and drain current (I_{DS}). This remarkable mechanical stability is primarily due to the improved interface quality and reduced interface state density, making these devices highly suitable for flexible electronic applications [Figure 9B][67]. The incorporation of micro-hole arrays in thin metal films has been demonstrated as an effective method to mitigate mechanical stress. The micro-holes act as stress concentrators, localizing and controlling crack propagation, thereby preventing catastrophic failure of the electrodes. In the study by Lee *et al.* aluminum thin film electrodes with 3 μm diameter holes covering 25% of the area showed remarkable durability, maintaining less than a 3% change in resistance after 300,000 bending cycles. The electrical performance of a-IGZO TFTs with this micro-hole structure remained stable even after 10,000 bending cycles, indicating that the micro-hole arrays

Table 7. The summarization of MO TFTs employing device structures for mechanical flexibility

Structure	Channel materials	Substrate	Buffer layer	T_{max} (°C)	Bending radius (mm)	μ_{FE} ($cm^2 \cdot V^{-1} \cdot s^{-1}$)	SS (V/decade)	On/off ratio	Gate dielectric	Refs.	Year
Island	IGZO	TPU	Al_2O_3	200	1.5	10.9	0.33	10^8	Al_2O_3	[102]	2021
	IGZO	PI	SiN_x/SiO_2	450	1	14	-	10^7	SiO_2	[193]	2016
	IGZO	PI	Al_2O_3	150	0.125	6.06	-	-	Al_2O_3	[33]	2020
	ITZO	PI	Polymer	300	-	30	-	10^8	SiO_2	[199]	2022
	IGZO	PDMS	-	200	-	6.1	-	10^7	P(VDF-TrFE):PMMA	[124]	2015
Junctionless	ITO	Paper	-	70	-	2.3	0.11	10^5	Chitosan	[66]	2021
	ITO	Paper	-	-	-	-	0.21	10^6	SiO_2 solid electrolyte	[64]	2012
	ITO	Paper	-	-	-	12.8	-	10^7	Chitosan	[194]	2019
	IZO	PET	-	-	20	60	0.13	10^6	SiO_2 solid electrolyte	[65]	2013
	ITO	PI	-	200	0.125	12.74	0.881	10^7	Al_2O_3	[198]	2024
Electrode and channel architecture	IGZO	PI	SiO_2/SiN_x	450	0.32	14.3	0.39	-	SiO_2/SiN_x	[61]	2017
	IGZO	PI	SiO_2/SiN_x	450	1	76.8	0.077		SiO_2/SiN_x	[67]	2017
	IGZO	PI	-	300	5	5	0.8	10^7	-	[62]	2020

MO: Metal oxide; TFTs: thin-film transistors; SS: subthreshold swing; IGZO: indium gallium zinc oxide; TPU: thermoplastic polyurethane; PI: polyimide; ITZO: indium tin zinc oxide; PDMS: polydimethylsiloxane; ITO: indium-tin-oxide; IZO: indium zinc oxide; PET: polyethylene terephthalate.

do not significantly degrade the electrical properties of the TFTs. The stress distribution simulations showed that without holes, the stress is uniformly distributed across the film, leading to random crack formation under bending. With holes, stress is localized around the hole edges, which can be controlled to prevent random propagation. This strategy enhances the durability of metal electrodes under mechanical strain, making it suitable for various flexible electronic applications. The a-IGZO TFTs with hole arrays not only exhibit improved mechanical stability but also maintain comparable electrical performance to standard TFTs, demonstrating the feasibility of micro-hole structures in practical devices [Figure 9C][62].

Both the micro-hole array and mesh structure approaches offer significant improvements in the mechanical robustness of flexible TFTs. The micro-hole arrays focus on localizing stress and controlling crack propagation, which is particularly effective for metal electrodes and oxide TFTs. On the other hand, the mesh structures provide an even distribution of stress across the device, enhancing overall mechanical stability. These strategies can be combined or further optimized to develop even more resilient flexible electronic devices. Lastly, we summarized properties of MO TFTs with device structures designed for mechanical flexibility in Table 7.

Future research could explore the integration of these designs with advanced materials and fabrication techniques to further enhance the performance and durability of flexible electronics. Additionally, the impact of different hole shapes, sizes, and patterns on the mechanical and electrical properties of the devices can be investigated to fine-tune the design for specific applications. The goal is to develop flexible electronics that can withstand the rigors of real-world use while maintaining high performance.

APPLICATION

Flexible displays

Flexible MO TFTs have become essential for developing next-generation display technologies, including VR, AR, and flexible devices. The mechanical flexibility and superior electrical properties of MO semiconductors have opened new possibilities for flexible, foldable, and rollable display applications.

Recent advancements in high-performance flexible displays involve the integration of ITZO TFTs and air-stable inverted OLEDs (iOLEDs). For instance, ITZO TFTs fabricated on PI films exhibit high mobility (32.9 $cm^2 \cdot V^{-1} \cdot s^{-1}$) and stability. This technology enables high-resolution displays suitable for next-generation flexible applications by simplifying the fabrication process through the simultaneous formation of ITZO films as both the channel layer in TFTs and electron injection layers in iOLEDs [Figure 10A][200]. Additionally, a flexible green AMOLED display with a resolution of 320 × 3 × 240 pixels (80 ppi resolution) has been developed. The flexible AMOLED display is integrated on the flexible TFT panel on a PEN substrate. Each pixel driver circuit consists of two TFTs and a storage capacitor, providing an aperture ratio of 46%. This TFT consists of an Al:Nd gate electrode, an AlOx:Nd gate dielectric, an IGZO channel, ITO S/D electrodes, and an SU-8 passivation layer. The display achieves 250 cd/m^2 in both flat and bent conditions, maintaining clear image quality without significant luminance degradation or visible defects even when bent to a 20 mm bending radius [Figure 10B][201].

Flexible circuits

Flexible MO TFTs are also crucial in developing various electronic circuits integrated into flexible devices. These devices have the ability to fabricate island structure and junctionless TFTs while maintaining high performance under mechanical stress. Island structure TFTs distribute mechanical stress evenly, preventing the concentration of mechanical stress in any one area. Junctionless TFTs eliminate source/drain-to-channel junctions, reducing the risk of performance degradation under mechanical stress.

Innovative research has led to the development of flexible circuits that withstand significant mechanical deformation. DGTFTs on paper substrates using solution-processed chitosan-based proton conductors as the gate dielectric have been developed. Employing a dual gate enables precise modulation of the threshold voltage and facilitates logic operations. DGTFTs exhibited stable performance and switching characteristics. For the logic function of junctionless DGTFTs, various voltage pulses were applied to the dual in-plane gates, serving as inputs, while the drain/source current (I_{DS}) was used as the output. The voltages of -1 and 0 V represent the low and high inputs, respectively. This operation is characteristic of an AND logic gate, maintaining a consistent on/off current ratio of approximately 10^6 without a decrease in on current [Figure 8B][194]. Flexible circuits utilizing MO TFTs have achieved significant advancements, combining high performance with mechanical robustness. Mesa-island structures have enabled the creation of seven-stage ring oscillators with a-IGZO TFTs, which maintain stable operation even after repeated bending. This design allows for high-density integration and stress relaxation, making these flexible circuits ideal for applications in wearable devices, flexible displays, and portable electronics [Figure 11A][33]. Another noteworthy advancement is the hardwired machine learning processing engine fabricated with submicron metal-oxide TFTs on a flexible substrate. This device integrates AI capabilities into flexible electronics, offering robust performance and flexibility. It is designed to efficiently handle machine learning tasks, making it suitable for smart, adaptive wearable devices and flexible AI systems [Figure 11B][37]. Recent developments include a natively flexible 32-bit Arm microprocessor, which integrates complex computational functionalities into a flexible format. This microprocessor, fabricated on a flexible substrate, demonstrates operational stability under significant mechanical deformation, showcasing the potential of flexible electronics in advanced computing applications such as wearable technology and flexible computing devices [Figure 11C][36]. Papadopoulos *et al.* exhibited touchscreen tags utilizing thin-film electronics, aimed

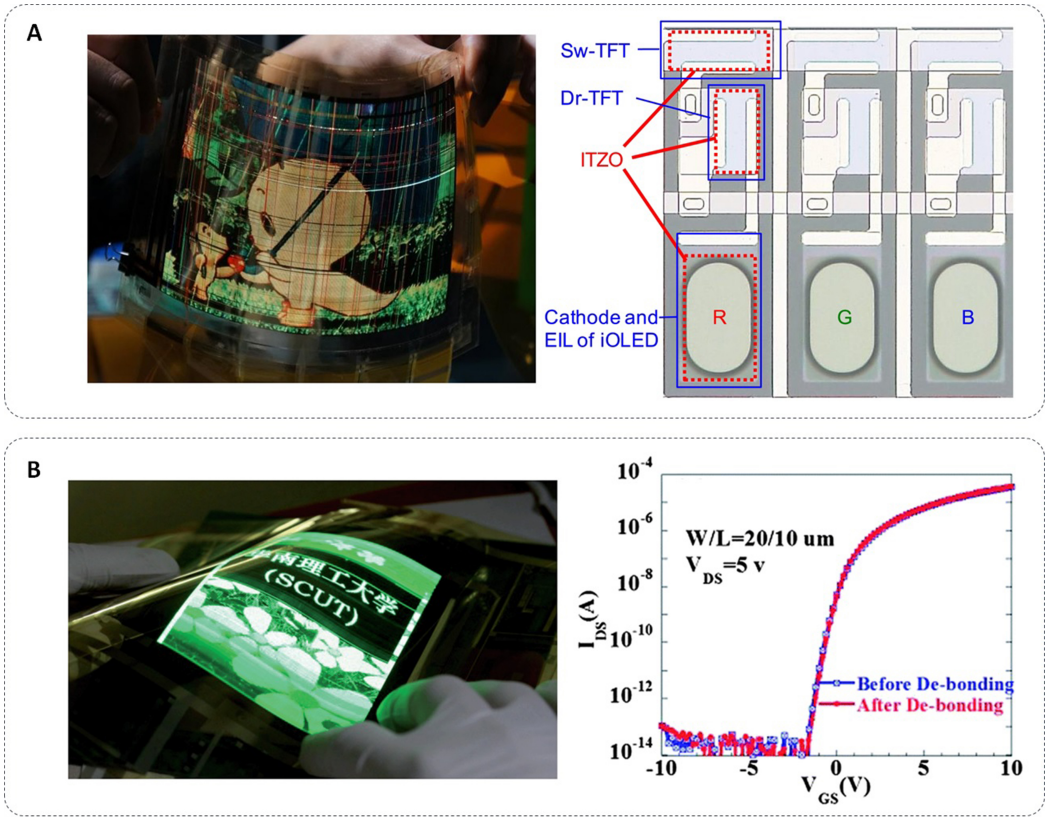

Figure 10. Flexible display employing high-performance flexible MO TFTs. (A) Photograph of flexible display with ITZO TFTs and ITZO-based iOLED. Microscopic image of pixel employing flexible ITZO TFTs backplane with ITO cathode and ITZO electron injection layer of the iOLED. Reproduced with permission[200]. Copyright 2016, Society for Information Display; (B) Flexible bottom emission green AMOLED display on PEN substrate using flexible a-IGZO TFTs. Transfer characteristics of flexible IGZO TFTs before and after bending. Reproduced with permission[201]. Copyright 2014, The Royal Society of Chemistry. MO: Metal oxide; TFTs: thin-film transistors; ITZO: indium tin zinc oxide; iOLED: inverted organic light-emitting diodes; ITO: indium-tin-oxide; AMOLED: active-matrix organic light-emitting diode; PEN: polyethylene naphthalate.

at enhancing connectivity in the Internet of Everything (IoE). These flexible touchscreen tags can be embedded in various objects, enabling interactive features and connectivity. The tags demonstrate excellent mechanical flexibility and reliable performance, showing promise for widespread application in smart packaging, interactive labels, and ubiquitous IoE devices [Figure 11D][35].

CONCLUSION AND OUTLOOK

In summary, MO TFTs are at the forefront of the advancement of flexible display technologies, poised to play a critical role in the next generation of wearable and soft electronics. The inherent advantages of MO semiconductors, such as high carrier mobility, low processing temperatures, excellent electrical uniformity, transparency to visible light, and cost-effectiveness, make them particularly suitable for these applications. Their well-established and matured large-scale processes in the traditional display industry and compatibility with CMOS processes further underpin their potential for broader applications, including integrated circuits for wearable and soft electronics.

Recent research has made significant advances in the mechanical flexibility and electrical performance of MO TFTs, which are crucial for the development of ultra-high-resolution AR/VR displays and complex integrated circuits such as microprocessors. This review has identified the principal developments in

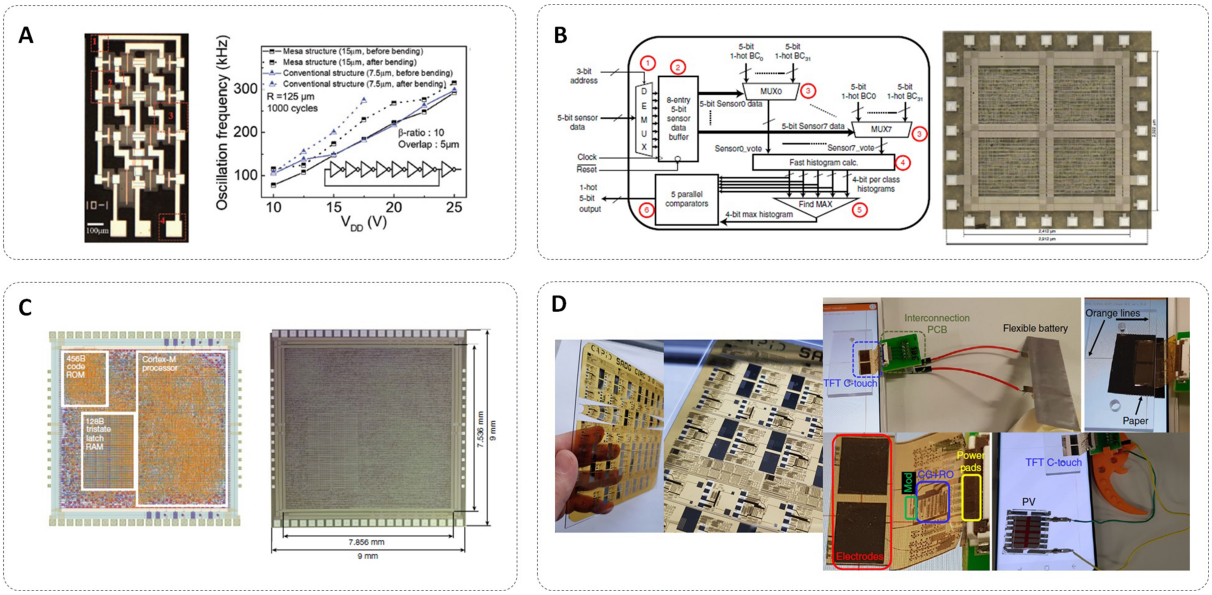

Figure 11. Flexible circuit employing flexible MO TFTs. (A) optical image of solution-processed IGZO TFTs employing island structure on a PI substrate. Oscillation frequency of flexible solution-processed IGZO TFTs ring oscillator as a function of supply voltage. Reproduced with permission[33]. Copyright 2020, Wiley-VCH; (B) The microarchitecture of UB-FVC inference stage. Microimage of the natively flexible processing engine implementing UB-FVC microarchitecture. Reproduced with permission[37]. Copyright 2020, Springer Nature; (C) The die layout of PlasticARM, denoting the key blocks in white boxes. The die micro image of PlasticARM, showing the dimensions of the die and core areas. Reproduced with permission[36]. Copyright 2020, Springer Nature; (D) Photo image of a quarter of a GEN1 (350 mm × 320 mm) plastic substrate and flexible touchscreen tag connected to a flexible battery on an iPhone Reproduced with permission[35]. Copyright 2020, Springer Nature. MO: Metal oxide; TFTs: thin-film transistors; IGZO: indium gallium zinc oxide; PI: polyimide; UB-FVC: univariate Bayes feature voting classifier.

materials, fabrication processes, and device architecture engineering methods that underpin these improvements. The functional layers of high-performance flexible MO TFTs, including gate dielectrics, single MO channel layers, and multiple MO channel layers, directly influence carrier transport and electrical properties. The incorporation of innovative materials and the utilization of multiple layers, including LiZnO, ZnON, and Al-ITZO, which demonstrate enhanced field-effect mobility compared to IGZO, have led to an improvement in the electrical performance of flexible MO TFTs. The incorporation of heterojunction layers and high-k dielectrics, which combine MOs and polymers, has further enhanced the electrical performance and mechanical stability of the devices. Moreover, doping processes, such as nitrogen and hydrogen doping, have been demonstrated to improve the electrical performance of flexible MO TFTs while maintaining compatibility with low-temperature fabrication methods, which are crucial for flexible substrates. Recent mechanical bending tests have demonstrated the robust functionality of high-performance flexible MO TFTs under various bending radii. This has been achieved with innovative structures, including island structures, junctionless structures, and advanced S/D electrode architectures. Island structures localize mechanical strain, preventing damage. Junctionless structures simplify device architecture and improve mechanical robustness. Advanced electrode designs ensure consistent electrical performance under significant mechanical deformation. The review also describes applications of high-performance flexible MO TFTs in flexible electronic systems, including displays and integrated circuits.

Despite these advances, several challenges remain to be addressed in future research to fully realize the potential of MO-TFT-based flexible displays and electronics:

1. Development of p-type MO semiconductors for CMOS implementation: To fully realize the potential applications of oxide TFT technology, it is imperative to develop high-performance p-type MO semiconductors. This advancement would enable the fabrication of CMOS circuits, allowing flexible electronics to benefit from increased scalability and integration density, reduced power dissipation, improved noise immunity, and versatile functionalities characteristic of modern advanced integrated circuits.

2. Downscaling and short-channel devices for high-performance integrated circuits: To meet the demands of high-performance and highly integrated circuits, future research should focus on downscaling MO TFTs and developing short-channel devices. Techniques such as self-alignment and double-gate structures can improve device performance and scalability. In addition, the development of low-cost, high-resolution patterning methods is essential to ensure that these advanced devices can be manufactured economically and with the precision required for low-cost, high-density integration.

3. Stretchable integrated systems beyond flexibility: Extending the current capabilities of flexible MO TFTs to stretchable systems will pave the way for more robust and versatile applications in wearables and soft electronics. This will require the development of materials and architectures that can withstand significant mechanical deformation while maintaining high performance.

4. Integration with emerging display technologies: Future research should explore the integration of flexible and stretchable MO-TFT backplanes with next-generation display technologies such as colloidal quantum dot light-emitting diodes (LEDs), perovskite LEDs, and colloidal quantum well LEDs. This would facilitate the development of advanced integrated systems for next-generation flexible displays.

By addressing these challenges, the potential of flexible MO TFTs can be fully realized, leading to significant advances in the field of flexible and stretchable displays and electronics. Looking ahead, continued innovation in MO TFT technology promises to unlock new opportunities in next-generation electronics. Leveraging the mature processes of MO TFTs offers a cost-effective approach that can potentially complement or even replace traditional silicon-based semiconductors. The lower processing temperature of oxide TFTs compared to silicon makes them compatible with BEOL processing for M3D integration on existing silicon CMOS chips. This compatibility allows for increased packing density of transistors and other components, enabling the development of more powerful and compact electronic devices within a smaller footprint. Consequently, the integration of MO TFTs into multifunctional and novel applications beyond display technologies has the potential to revolutionize the design and functionality of future electronic devices.

DECLARATIONS

Authors' contributions

Initiated the reviewing idea and outlined the manuscript structure: Jeon, S.P., Jo, J.W., Kim, Y.H., Park, S.K.
Conducted the literature review and wrote the manuscript: Jeon, S.P., Jo, J.W., Nam, D., Kim, Y.H., Park, S.K.
Involved in the discussion and revised the manuscript: Jeon, S.P., Jo, J.W., Kim, Y.H., Park, S.K.
Supervision, review and editing, and project administration: Kim, Y.H., Park, S.K.

Availability of data and materials

Not applicable.

Financial support and sponsorship

This work was supported by the Korea Institute for Advancement of Technology (KIAT) grant funded by the Korea Government (MOTIE) (P0023718, Inorganic Light-emtting Display Expert Training Program for Display Technology Transition), the KIAT grant funded by the Korea Government (MOTIE) (P0020967, Advanced Training Program for Smart Sensor Engineers), and the Technology Innovation Program (Development of application product in foam-based adhesive sheet with high impact resistance, 20022424) funded by the Ministry of Trade, Industry & Energy (MOTIE, Korea).

Conflicts of interest

Park, S.K. is the guest editor of the special issue, while the other authors have declared that they have no conflicts of interest.

Ethical approval and consent to participate

Not applicable.

Consent for publication

Not applicable.

REFERENCES

1. Myny, K. The development of flexible integrated circuits based on thin-film transistors. *Nat. Electron.* **2018**, *1*, 30-9. DOI
2. Ohshima, H. Mobile display technologies: past developments, present technologies, and future opportunities. *Jpn. J. Appl. Phys.* **2014**, *53*, 03CA01. DOI
3. Hwang, T.; Yang, I.; Kwon, O.; et al. Inverters using only N-type indium gallium zinc oxide thin film transistors for flat panel display applications. *Jpn. J. Appl. Phys.* **2011**, *50*, 03CB06. DOI
4. Chung, K.; Hong, M. P.; Kim, C. W.; Kang, I. Needs and solutions of future flat panel display for information technology industry. In: Digest. International Electron Devices Meeting; 2002 Dec 08-11; San Francisco, USA. IEEE; 2002. pp. 385-8. DOI
5. Fukuda, K.; Someya, T. Recent progress in the development of printed thin-film transistors and circuits with high-resolution printing technology. *Adv. Mater.* **2017**, *29*, 1602736. DOI PubMed
6. Zhang, G.; Xu, Y.; Haider, M.; Sun, J.; Zhang, D.; Yang, J. Printing flexible thin-film transistors. *Appl. Phys. Rev.* **2023**, *10*, 031313. DOI
7. Acharya, V.; Agarwal, K.; Mondal, S. Electronic materials for solution-processed TFTs. *Mater. Res. Express.* **2023**, *10*, 082002. DOI
8. Park, J. W.; Kang, B. H.; Kim, H. J. A review of low-temperature solution-processed metal oxide thin-film transistors for flexible electronics. *Adv. Funct. Mater.* **2020**, *30*, 1904632. DOI
9. Street, R. A. Thin-film transistors. *Adv. Mater.* **2009**, *21*, 2007-22. DOI
10. Cantarella, G.; Costa, J.; Meister, T.; et al. Review of recent trends in flexible metal oxide thin-film transistors for analog applications. *Flex. Print. Electron.* **2020**, *5*, 033001. DOI
11. Fortunato, E.; Barquinha, P.; Martins, R. Oxide semiconductor thin-film transistors: a review of recent advances. *Adv. Mater.* **2012**, *24*, 2945-86. DOI PubMed
12. Petti, L.; Münzenrieder, N.; Vogt, C.; et al. Metal oxide semiconductor thin-film transistors for flexible electronics. *Appl. Phys. Rev.* **2016**, *3*, 021303. DOI
13. Kimura, M. Emerging applications using metal-oxide semiconductor thin-film devices. *Jpn. J. Appl. Phys.* **2019**, *58*, 090503. DOI
14. Nomura, K.; Ohta, H.; Takagi, A.; Kamiya, T.; Hirano, M.; Hosono, H. Room-temperature fabrication of transparent flexible thin-film transistors using amorphous oxide semiconductors. *Nature* **2004**, *432*, 488-92. DOI PubMed
15. Panca, A.; Panidi, J.; Faber, H.; Stathopoulos, S.; Anthopoulos, T. D.; Prodromakis, T. Flexible oxide thin film transistors, memristors, and their integration. *Adv. Funct. Mater.* **2023**, *33*, 2213762. DOI
16. Park, J. S.; Maeng, W.; Kim, H.; Park, J. Review of recent developments in amorphous oxide semiconductor thin-film transistor devices. *Thin. Solid. Films.* **2012**, *520*, 1679-93. DOI
17. Heremans, P.; Tripathi, A. K.; de, J. M. A.; et al. Mechanical and electronic properties of thin-film transistors on plastic, and their integration in flexible electronic applications. *Adv. Mater.* **2016**, *28*, 4266-82. DOI PubMed
18. Sanctis, S. Multinary metal oxide semiconductors - A study of different material systems and their application in thin-film transistors. 2020. DOI

19. Bonnassieux, Y.; Brabec, C. J.; Cao, Y.; et al. The 2021 flexible and printed electronics roadmap. *Flex. Print. Electron.* **2021**, *6*, 023001. DOI
20. Choi, M. K.; Yang, J.; Hyeon, T.; Kim, D. Flexible quantum dot light-emitting diodes for next-generation displays. *npj. Flex. Electron.* **2018**, *2*, 23. DOI
21. Zhang, D.; Huang, T.; Duan, L. Emerging self-emissive technologies for flexible displays. *Adv. Mater.* **2020**, *32*, e1902391. DOI PubMed
22. Jeon, Y.; Lee, D.; Yoo, H. Recent advances in metal-oxide thin-film transistors: flexible/stretchable devices, integrated circuits, biosensors, and neuromorphic applications. *Coatings* **2022**, *12*, 204. DOI
23. Jo, J. W.; Kang, S. H.; Heo, J. S.; Kim, Y. H.; Park, S. K. Flexible metal oxide semiconductor devices made by solution methods. *Chemistry* **2020**, *26*, 9126-56. DOI PubMed
24. Kim, J.; Jo, C.; Kim, M. G.; et al. Vertically stacked full color quantum dots phototransistor arrays for high-resolution and enhanced color-selective imaging. *Adv. Mater.* **2022**, *34*, e2106215. DOI PubMed
25. Jang, Y. W.; Kim, J.; Shin, J.; et al. Autonomous artificial olfactory sensor systems with homeostasis recovery via a seamless neuromorphic architecture. *Adv. Mater.* **2024**, *36*, e2400614. DOI PubMed
26. Zhang, X.; Ju, E. C.; Lee, J. M.; Park, S. K.; Cho, S. W. Ultraviolet-sensitive and power-efficient oxide phototransistor enabled by nanometer-scale thickness engineering of InZnO semiconductor and gate bias modulation. *Appl. Phys. Lett.* **2023**, *123*, 261104. DOI
27. Kang, S. H.; Jo, J. W.; Lee, J. M.; et al. Full integration of highly stretchable inorganic transistors and circuits within molecular-tailored elastic substrates on a large scale. *Nat. Commun.* **2024**, *15*, 2814. DOI PubMed PMC
28. Jang, Y.; Kang, J.; Jo, J.; Kim, Y.; Kim, J.; Park, S. K. Improved dynamic responses of room-temperature operable field-effect-transistor gas sensors enabled by programmable multi-spectral ultraviolet illumination. *Sensor. Actuat. B. Chem.* **2021**, *342*, 130058. DOI
29. Kim, J.; Kwon, S. M.; Kang, Y. K.; et al. A skin-like two-dimensionally pixelized full-color quantum dot photodetector. *Sci. Adv.* **2019**, *5*, eaax8801. DOI PubMed PMC
30. Kim, K.; Kang, S.; Kim, J.; Heo, J. S.; Kim, Y.; Park, S. K. An ultra-flexible solution-processed metal-oxide/carbon nanotube complementary circuit amplifier with highly reliable electrical and mechanical stability. *Adv. Elect. Mater.* **2020**, *6*, 1900845. DOI
31. Jo, C.; Lee, S.; Kim, J.; Heo, J. S.; Kang, D. W.; Park, S. K. Enhanced electro-optical performance of inorganic perovskite/a-InGaZnO phototransistors enabled by Sn-Pb binary incorporation with a selective photonic deactivation. *ACS. Appl. Mater. Interfaces.* **2020**, *12*, 58038-48. DOI PubMed
32. Kim, K.; Lee, K. W.; Kang, S.; et al. Stress-released amorphous oxide/carbon nanotube CMOS amplifier circuits for skin-compatible electronics. *ACS. Appl. Electron. Mater.* **2021**, *3*, 4950-8. DOI
33. Kim, K. T.; Moon, S.; Kim, M.; et al. Highly scalable and robust mesa-island-structure metal-oxide thin-film transistors and integrated circuits enabled by stress-diffusive manipulation. *Adv. Mater.* **2020**, *32*, e2003276. DOI PubMed
34. Kim, J.; Song, S.; Lee, J. M.; et al. Metal-oxide heterojunction optoelectronic synapse and multilevel memory devices enabled by broad spectral photocarrier modulation. *Small* **2023**, *19*, e2301186. DOI PubMed
35. Papadopoulos, N.; Qiu, W.; Ameys, M.; et al. Touchscreen tags based on thin-film electronics for the Internet of Everything. *Nat. Electron.* **2019**, *2*, 606-11. DOI PubMed PMC
36. Biggs, J.; Myers, J.; Kufel, J.; et al. A natively flexible 32-bit Arm microprocessor. *Nature* **2021**, *595*, 532-6. DOI PubMed
37. Ozer, E.; Kufel, J.; Myers, J.; et al. A hardwired machine learning processing engine fabricated with submicron metal-oxide thin-film transistors on a flexible substrate. *Nat. Electron.* **2020**, *3*, 419-25. DOI
38. Jo, C.; Kim, J.; Kwak, J. Y.; et al. Retina-inspired color-cognitive learning via chromatically controllable mixed quantum dot synaptic transistor arrays. *Adv. Mater.* **2022**, *34*, e2108979. DOI PubMed
39. Kwon, S. M.; Kwak, J. Y.; Song, S.; et al. Large-area pixelized optoelectronic neuromorphic devices with multispectral light-modulated bidirectional synaptic circuits. *Adv. Mater.* **2021**, *33*, e2105017. DOI PubMed
40. Kwon, S. M.; Kang, S.; Cho, S. S.; et al. Bidirectionally modulated synaptic plasticity with optically tunable ionic electrolyte transistors. *ACS. Appl. Electron. Mater.* **2022**, *4*, 2629-35. DOI
41. Cho, S. W.; Jo, C.; Kim, Y. H.; Park, S. K. Progress of materials and devices for neuromorphic vision sensors. *Nanomicro. Lett.* **2022**, *14*, 203. DOI PubMed PMC
42. Cho, S. S.; Kim, J.; Jeong, S.; et al. Highly adaptive and energy efficient neuromorphic computation enabled by deep-spike heterostructure photonic neuro-transistors. *Nano. Energy.* **2022**, *104*, 107991. DOI
43. Kang, C.; Lee, H. Recent progress of organic light-emitting diode microdisplays for augmented reality/virtual reality applications. *J. Inform. Display.* **2022**, *23*, 19-32. DOI
44. Li, W.; Geng, D.; Yang, G.; Lu, N.; Li, L. Review of nanoscale oxide thin-film transistors for emerging display and memory applications. *IEEE. Open. J. Immers. Disp.* **2024**, *1*, 51-61. DOI
45. Si, M.; Lin, Z.; Chen, Z.; Sun, X.; Wang, H.; Ye, P. D. Scaled indium oxide transistors fabricated using atomic layer deposition. *Nat. Electron.* **2022**, *5*, 164-70. DOI
46. Zhu, J.; Park, J. H.; Vitale, S. A.; et al. Low-thermal-budget synthesis of monolayer molybdenum disulfide for silicon back-end-of-line integration on a 200 mm platform. *Nat. Nanotechnol.* **2023**, *18*, 456-63. DOI
47. Zhang, J.; Wang, W.; Zhu, J.; et al. Ultra-flexible monolithic 3D complementary metal-oxide-semiconductor electronics. *Adv. Funct. Mater.* **2023**, *33*, 2305379. DOI

48. Hua, Q.; Shen, G. Low-dimensional nanostructures for monolithic 3D-integrated flexible and stretchable electronics. *Chem. Soc. Rev.* **2024**, *53*, 1316-53. DOI
49. Wang, X.; Qi, L.; Yang, H.; Rao, Y.; Chen, H. Stretchable synaptic transistors based on the field effect for flexible neuromorphic electronics. *Soft. Sci.* **2023**, *3*, 15. DOI
50. Na, B. S.; Jung, S.; Moon, Y. G.; et al. InGaZnO-based stretchable ferroelectric memory transistor using patterned polyimide/polydimethylsiloxane hybrid substrate. *J. Nanosci. Nanotechnol.* **2016**, *16*, 10280-3. DOI
51. Cantarella, G.; Costanza, V.; Ferrero, A.; et al. Design of engineered elastomeric substrate for stretchable active devices and sensors. *Adv. Funct. Mater.* **2018**, *28*, 1705132. DOI
52. Park, K.; Lee, D.; Kim, B.; et al. Stretchable, transparent zinc oxide thin film transistors. *Adv. Funct. Mater.* **2010**, *20*, 3577-82. DOI
53. Kim, Y. H.; Lee, E.; Um, J. G.; Mativenga, M.; Jang, J. Highly robust neutral plane oxide TFTs withstanding 0.25 mm bending radius for stretchable electronics. *Sci. Rep.* **2016**, *6*, 25734. DOI PubMed PMC
54. Kim, J. O.; Hur, J. S.; Kim, D.; et al. Network structure modification-enabled hybrid polymer dielectric film with zirconia for the stretchable transistor applications. *Adv. Funct. Mater.* **2020**, *30*, 1906647. DOI
55. Parthiban, S.; Kwon, J. Y. Role of dopants as a carrier suppressor and strong oxygen binder in amorphous indium-oxide-based field effect transistor. *J. Mater. Res.* **2014**, *29*, 1585-96. DOI
56. Heo, J. S.; Jeon, S. P.; Kim, I.; Lee, W.; Kim, Y. H.; Park, S. K. Suppression of interfacial disorders in solution-processed metal oxide thin-film transistors by Mg doping. *ACS. Appl. Mater. Interfaces.* **2019**, *11*, 48054-61. DOI PubMed
57. Jeon, S. P.; Heo, J. S.; Kim, I.; Kim, Y. H.; Park, S. K. Enhanced interfacial integrity of amorphous oxide thin-film transistors by elemental diffusion of ternary oxide semiconductors. *ACS. Appl. Mater. Interfaces.* **2020**, *12*, 57996-8004. DOI PubMed
58. Li, H.; Qu, M.; Zhang, Q. Influence of tungsten doping on the performance of indium–zinc–oxide thin-film transistors. *IEEE. Electron. Device. Lett.* **2013**, *34*, 1268-70. DOI
59. Lee, J.; Choi, C. H.; Kim, T.; et al. Hydrogen-doping-enabled boosting of the carrier mobility and stability in amorphous IGZTO transistors. *ACS. Appl. Mater. Interfaces.* **2022**, *14*, 57016-27. DOI
60. Banger, K. K.; Peterson, R. L.; Mori, K.; Yamashita, Y.; Leedham, T.; Sirringhaus, H. High performance, low temperature solution-processed barium and strontium doped oxide thin film transistors. *Chem. Mater.* **2014**, *26*, 1195-203. DOI PubMed PMC
61. Lee, S.; Jeong, D.; Mativenga, M.; Jang, J. Highly robust bendable oxide thin-film transistors on polyimide substrates via mesh and strip patterning of device layers. *Adv. Funct. Mater.* **2017**, *27*, 1700437. DOI
62. Lee, G. J.; Heo, S. J.; Lee, S.; et al. Stress release effect of micro-hole arrays for flexible electrodes and thin film transistors. *ACS. Appl. Mater. Interfaces.* **2020**, *12*, 19226-34. DOI PubMed
63. Yuan, X.; Dou, W.; Gan, X.; et al. Junctionless electric-double-layer thin-film transistors with logic functions. *Phys. Status. Solidi. RRL.* **2023**, *17*, 2200480. DOI
64. Jiang, J.; Sun, J.; Dou, W.; Wan, Q. Junctionless flexible oxide-based thin-film transistors on paper substrates. *IEEE. Electron. Device. Lett.* **2012**, *33*, 65-7. DOI
65. Zhou, J.; Wu, G.; Guo, L.; Zhu, L.; Wan, Q. Flexible transparent junctionless TFTs With oxygen-tuned indium-zinc-oxide channels. *IEEE. Electron. Device. Lett.* **2013**, *34*, 888-90. DOI
66. Yuan, X.; Tan, Y.; Lei, L.; et al. Junctionless electric-double-layer TFTs on paper substrate. *ECS. J. Solid. State. Sci. Technol.* **2021**, *10*, 045004. DOI
67. Lee, S.; Shin, J.; Jang, J. Top interface engineering of flexible oxide thin-film transistors by splitting active layer. *Adv. Funct. Mater.* **2017**, *27*, 1604921. DOI
68. Nakata, M.; Takechi, K.; Eguchi, T.; Tokumitsu, E.; Yamaguchi, H.; Kaneko, S. Effects of thermal annealing on ZnO thin-film transistor characteristics and the application of excimer laser annealing in plastic-based ZnO thin-film transistors. *Jpn. J. Appl. Phys.* **2009**, *48*, 081608. DOI
69. Zhang, J.; Liu, Y.; Guo, L.; et al. Flexible oxide-based thin-film transistors on plastic substrates for logic applications. *J. Mater. Sci. Technol.* **2015**, *31*, 171-4. DOI
70. Cantarella, G.; Ishida, K.; Petti, L.; et al. Flexible In–Ga–Zn–O-based circuits with two and three metal layers: simulation and fabrication study. *IEEE. Electron. Device. Lett.* **2016**, *37*, 1582-5. DOI
71. Song, K.; Noh, J.; Jun, T.; Jung, Y.; Kang, H. Y.; Moon, J. Fully flexible solution-deposited zno thin-film transistors. *Adv. Mater.* **2010**, *22*, 4308-12. DOI PubMed
72. Rim, Y. S.; Chen, H.; Liu, Y.; Bae, S. H.; Kim, H. J.; Yang, Y. Direct light pattern integration of low-temperature solution-processed all-oxide flexible electronics. *ACS. Nano.* **2014**, *8*, 9680-6. DOI PubMed
73. Bong, H.; Lee, W. H.; Lee, D. Y.; Kim, B. J.; Cho, J. H.; Cho, K. High-mobility low-temperature ZnO transistors with low-voltage operation. *Appl. Phys. Lett.* **2010**, *96*, 192115. DOI
74. Lim, W.; Jang, J. H.; Kim, S.; et al. High performance indium gallium zinc oxide thin film transistors fabricated on polyethylene terephthalate substrates. *Appl. Phys. Lett.* **2008**, *93*, 082102. DOI
75. Han, D.; Chen, Z.; Cong, Y.; Yu, W.; Zhang, X.; Wang, Y. High-performance flexible tin-zinc-oxide thin-film transistors fabricated on plastic substrates. *IEEE. Trans. Electron. Devices.* **2016**, *63*, 3360-3. DOI
76. Ha, Y. G.; Everaerts, K.; Hersam, M. C.; Marks, T. J. Hybrid gate dielectric materials for unconventional electronic circuitry. *Acc. Chem. Res.* **2014**, *47*, 1019-28. DOI PubMed
77. Smith, J. T.; Shah, S. S.; Goryll, M.; Stowell, J. R.; Allee, D. R. Flexible ISFET biosensor using IGZO metal oxide TFTs and an ITO

sensing layer. *IEEE. Sensors. J.* **2014**, *14*, 937-8. DOI

78. Kim, S.; Park, M.; Yun, D.; Lee, W.; Kim, G.; Yoon, S. High performance and stable flexible memory thin-film transistors using In–Ga–Zn–O channel and ZnO charge-trap layers on poly(ethylene naphthalate) substrate. *IEEE. Trans. Electron. Devices.* **2016**, *63*, 1557-64. DOI
79. Kim, J.; Nam, T.; Lim, S. J.; et al. Atomic layer deposition ZnO:N flexible thin film transistors and the effects of bending on device properties. *Appl. Phys. Lett.* **2011**, *98*, 142113. DOI
80. Jin, S. H.; Kang, S. K.; Cho, I. T.; et al. Water-soluble thin film transistors and circuits based on amorphous indium-gallium-zinc oxide. *ACS. Appl. Mater. Interfaces.* **2015**, *7*, 8268-74. DOI PubMed
81. Cantarella, G.; Munzenrieder, N.; Petti, L.; et al. Flexible In–Ga–Zn–O thin-film transistors on elastomeric substrate bent to 2.3% strain. *IEEE. Electron. Device. Lett.* **2015**, *36*, 781-3. DOI
82. Hsu, H.; Chiu, Y.; Chiou, P.; Cheng, C. Improvement of dielectric flexibility and electrical properties of mechanically flexible thin film devices using titanium oxide materials fabricated at a very low temperature of 100°C. *J. Alloys. Compd.* **2015**, *643*, S133-6. DOI
83. Oh, H.; Cho, K.; Park, S.; Kim, S. Electrical characteristics of bendable a-IGZO thin-film transistors with split channels and top-gate structure. *Microelectron. Eng.* **2016**, *159*, 179-83. DOI
84. Kim, J.; Fuentes-hernandez, C.; Hwang, D.; Potscavage, J. W, Cheun H, Kippelen B. Vertically stacked hybrid organic–inorganic complementary inverters with low operating voltage on flexible substrates. *Org. Electron.* **2011**, *12*, 45-50. DOI
85. Jin, J.; Ko, J. H.; Yang, S.; Bae, B. S. Rollable transparent glass-fabric reinforced composite substrate for flexible devices. *Adv. Mater.* **2010**, *22*, 4510-5. DOI PubMed
86. Lim, W.; Douglas, E. A.; Kim, S.; et al. High mobility InGaZnO4 thin-film transistors on paper. *Appl. Phys. Lett.* **2009**, *94*, 072103. DOI
87. Martins, R.; Ferreira, I.; Fortunato, E. Electronics with and on paper. *Phys. Status. Solidi. RRL.* **2011**, *5*, 332-5. DOI
88. Choi, N.; Khan, S. A.; Ma, X.; Hatalis, M. Amorphous oxide thin film transistors with methyl siloxane based gate dielectric on paper substrate. *Electrochem. Solid. State. Lett.* **2011**, *14*, H247. DOI
89. Wu, G. D.; Zhang, J.; Wan, X. Junctionless coplanar-gate oxide-based thin-film transistors gated by Al_2O_3 proton conducting films on paper substrates. *Chinese. Phys. Lett.* **2014**, *31*, 108505. DOI
90. Mahmoudabadi, F.; Ma, X.; Hatalis, M. K.; Shah, K. N.; Levendusky, T. L. Amorphous IGZO TFTs and circuits on conformable aluminum substrates. *Solid. State. Electron.* **2014**, *101*, 57-62. DOI
91. Park, I.; Jeong, C.; Cho, I.; et al. Fabrication of amorphous InGaZnO thin-film transistor-driven flexible thermal and pressure sensors. *Semicond. Sci. Technol.* **2012**, *27*, 105019. DOI
92. Tang, X.; Zhao, Y.; Li, K.; et al. In situ growth of (−201) fiber-textured β-Ga_2O_3 semiconductor tape for flexible thin-film transistor. *Adv. Electron. Mater.* **2024**, 2400046. DOI
93. Hosono, H. Transparent oxide semiconductors: fundamentals and recent progress. In: Facchetti A, Marks TJ, editors. Transparent electronics: from synthesis to applications. Wiley; 2010. pp. 31-59. DOI
94. He, Y.; Wang, X.; Gao, Y.; Hou, Y.; Wan, Q. Oxide-based thin film transistors for flexible electronics. *J. Semicond.* **2018**, *39*, 011005. DOI
95. Kim, H. J.; Park, K.; Kim, H. J. High-performance vacuum-processed metal oxide thin-film transistors: a review of recent developments. *J. Soc. Info. Display.* **2020**, *28*, 591-622. DOI
96. Zhang, X.; Wang, B.; Huang, W.; et al. Synergistic boron doping of semiconductor and dielectric layers for high-performance metal oxide transistors: interplay of experiment and theory. *J. Am. Chem. Soc.* **2018**, *140*, 12501-10. DOI PubMed
97. Nomura, K.; Kamiya, T.; Hirano, M.; Hosono, H. Origins of threshold voltage shifts in room-temperature deposited and annealed a-In–Ga–Zn–O thin-film transistors. *Appl. Phys. Lett.* **2009**, *95*, 013502. DOI
98. Bukke, R. N.; Mude, N. N.; Bae, J.; Jang, J. Nano-scale Ga_2O_3 interface engineering for high-performance of ZnO-based thin-film transistors. *ACS. Appl. Mater. Interfaces.* **2022**, *14*, 41508-19. DOI PubMed
99. Tang, T.; Dacha, P.; Haase, K.; et al. Analysis of the annealing budget of metal oxide thin-film transistors prepared by an aqueous blade-coating process. *Adv. Funct. Mater.* **2023**, *33*, 2207966. DOI
100. Lee, M.; Jo, J. W.; Kim, Y. J.; et al. Corrugated heterojunction metal-oxide thin-film transistors with high electron mobility via vertical interface manipulation. *Adv. Mater.* **2018**, *30*, e1804120. DOI PubMed
101. Bhatti, G.; Agrawal, Y.; Palaparthy, V.; Kavicharan, M.; Agrawal, M. Flexible electronics: a critical review. In: Agrawal Y, Mummaneni K, Sathyakam PU, editors. Interconnect technologies for integrated circuits and flexible electronics. Singapore: Springer Nature; 2024. pp. 221-48. DOI
102. Han, K.; Lee, W.; Kim, Y.; Kim, J.; Choi, B.; Park, J. Mechanical durability of flexible/stretchable a-IGZO TFTs on PI island for wearable electronic application. *ACS. Appl. Electron. Mater.* **2021**, *3*, 5037-47. DOI
103. Ribes, G.; Mitard, J.; Denais, M.; et al. Review on high-k dielectrics reliability issues. *IEEE. Trans. Device. Mater. Relib.* **2005**, *5*, 5-19. DOI
104. Choi, J.; Mao, Y.; Chang, J. Development of hafnium based high-k materials - a review. *Mat. Sci. Eng. R.* **2011**, *72*, 97-136. DOI
105. Wang, B.; Huang, W.; Chi, L.; Al-Hashimi, M.; Marks, T. J.; Facchetti, A. High-k gate dielectrics for emerging flexible and stretchable electronics. *Chem. Rev.* **2018**, *118*, 5690-754. DOI
106. Huang, X.; Jiang, P. Core-shell structured high-k polymer nanocomposites for energy storage and dielectric applications. *Adv. Mater.* **2015**, *27*, 546-54. DOI PubMed

107. Nadaud, N.; Lequeux, N.; Nanot, M.; Jové, J.; Roisnel, T. Structural studies of tin-doped indium oxide (ITO) and $In_4Sn_3O_{12}$. *J. Solid. State. Chem.* **1998**, *135*, 140-8. DOI
108. Sun, X.; Han, J.; Xiao, Z.; et al. High performance indium-tin-zinc-oxide thin-film transistor with hexamethyldisilazane passivation. *ACS. Appl. Electron. Mater.* **2024**, *6*, 2442-8. DOI
109. Kim, M. G.; Kim, H. S.; Ha, Y. G.; et al. High-performance solution-processed amorphous zinc-indium-tin oxide thin-film transistors. *J. Am. Chem. Soc.* **2010**, *132*, 10352-64. DOI PubMed
110. Ok, K. C.; Jeong, H. J.; Kim, H. S.; Park, J. S. Highly stable ZnON thin-film transistors with high field-effect mobility exceeding 50 cm^2/Vs. *IEEE. Electron. Device. Lett.* **2015**, *36*, 38-40. DOI
111. Tiwari, N.; Rajput, M.; John, R. A.; Kulkarni, M. R.; Nguyen, A. C.; Mathews, N. Indium tungsten oxide thin films for flexible high-performance transistors and neuromorphic electronics. *ACS. Appl. Mater. Interfaces.* **2018**, *10*, 30506-13. DOI PubMed
112. Chang, S.; Shih, S.; Lin, G. R. Amorphous hafnium-indium-zinc oxide semiconductor thin film transistors. *J. Nanomaterials.* **2012**, *2012*, 127646. DOI
113. Park, E.; Lee, H. M.; Kim, Y.; Jeong, H.; Park, J.; Park, J. Transparent flexible high mobility TFTs based on ZnON semiconductor with dual gate structure. *IEEE. Electron. Device. Lett.* **2020**, *41*, 401-4. DOI
114. Bukke R, Naik Mude N, Mobaidul Islam M, Jang J. Improvement of metal-oxide films by post atmospheric Ar/O_2 plasma treatment for thin film transistors with high mobility and excellent stability. *Appl. Surf. Sci.* **2021**, *568*, 150947. DOI
115. Shi, Y.; Shiah, Y.; Sim, K.; Sasase, M.; Kim, J.; Hosono, H. High-performance a-ITZO TFTs with high bias stability enabled by self-aligned passivation using a-GaOx. *Appl. Phys. Lett.* **2022**, *121*, 212101. DOI
116. Noh, J.; Kim, H.; Nahm, H.; et al. Cation composition effects on electronic structures of In-Sn-Zn-O amorphous semiconductors. *J. Appl. Phys.* **2013**, *113*, 183706. DOI
117. Ryu, M. K.; Yang, S.; Park, S. K.; Hwang, C.; Jeong, J. K. High performance thin film transistor with cosputtered amorphous Zn–In–Sn–O channel: combinatorial approach. *Appl. Phys. Lett.* **2009**, *95*, 072104. DOI
118. Li, T.; Liu, X.; Ren, J.; et al. High-mobility InSnZnO thin film transistors via introducing water vapor sputtering gas. *ACS. Appl. Mater. Interfaces.* **2024**, *16*, 31237-46. DOI PubMed
119. Ok, K. C.; Lim, J. H.; Jeong, H. J.; Lee, H. M.; Rim, Y. S.; Park, J. S. Photothermally activated nanocrystalline oxynitride with superior performance in flexible field-effect transistors. *ACS. Appl. Mater. Interfaces.* **2018**, *10*, 2709-15. DOI PubMed
120. Takagi, A.; Nomura, K.; Ohta, H.; et al. Carrier transport and electronic structure in amorphous oxide semiconductor, a-$InGaZnO_4$. *Thin. Solid. Films.* **2005**, *486*, 38-41. DOI
121. Lee, S.; Nathan, A.; Ye, Y.; Guo, Y.; Robertson, J. Localized tail states and electron mobility in amorphous ZnON thin film transistors. *Sci. Rep.* **2015**, *5*, 13467. DOI PubMed PMC
122. Kim, H. S.; Jeon, S. H.; Park, J. S.; et al. Anion control as a strategy to achieve high-mobility and high-stability oxide thin-film transistors. *Sci. Rep.* **2013**, *3*, 1459. DOI PubMed PMC
123. Park, C.; Jeon, S.; Park, J. B.; et al. High-performance ITO/a-IGZO heterostructure TFTs enabled by thickness-dependent carrier concentration and band alignment manipulation. *Ceram. Int.* **2023**, *49*, 5905-14. DOI
124. Jung, S. W.; Koo, J. B.; Park, C. W.; Na, B. S.; Oh, J. Y.; Lee, S. S. Fabrication of stretchable organic-inorganic hybrid thin-film transistors on polyimide stiff-island structures. *J. Nanosci. Nanotechnol.* **2015**, *15*, 7526-30. DOI PubMed
125. Lin, Y. H.; Faber, H.; Labram, J. G.; et al. High electron mobility thin-film transistors based on solution-processed semiconducting metal oxide heterojunctions and quasi-superlattices. *Adv Sci* 2015;2:1500058. DOI
126. Choi, I. M.; Kim, M. J.; On, N.; et al. Achieving high mobility and excellent stability in amorphous In–Ga–Zn–Sn–O thin-film transistors. *IEEE. Trans. Electron. Devices.* **2020**, *67*, 1014-20. DOI
127. Chang, Y.; Bukke, R. N.; Bae, J.; Jang, J. Low-temperature solution-processed HfZrO gate insulator for high-performance of flexible LaZnO thin-film transistor. *Nanomaterials* **2023**, *13*, 2410. DOI PubMed PMC
128. Liu, X.; Wang, C.; Cai, B.; et al. Rational design of amorphous indium zinc oxide/carbon nanotube hybrid film for unique performance transistors. *Nano. Lett.* **2012**, *12*, 3596-601. DOI
129. Divya, M.; Cherukupally, N.; Gogoi, S. K.; et al. Super flexible and high mobility inorganic/organic composite semiconductors for printed electronics on polymer substrates. *Adv. Mater. Technol.* **2023**, *8*, 2300256. DOI
130. Kim, K. S.; Kim, M. S.; Chung, J.; Kim, D.; Lee, I. S.; Kim, H. J. Polyimide-doped indium-gallium-zinc oxide-based transparent and flexible phototransistor for visible light detection. *ACS. Appl. Mater. Interfaces.* **2022**, *14*, 21150-8. DOI PubMed
131. Na, J. W.; Kim, H. J.; Hong, S.; Kim, H. J. Plasma polymerization enabled polymer/metal-oxide hybrid semiconductors for wearable electronics. *ACS. Appl. Mater. Interfaces.* **2018**, *10*, 37207-15. DOI PubMed
132. Lee, S.; Jeong, H.; Han, K.; Baek, G.; Park, J. An organic–inorganic hybrid semiconductor for flexible thin film transistors using molecular layer deposition. *J. Mater. Chem. C.* **2021**, *9*, 4322-9. DOI
133. Zhu, L.; Gao, Y.; Li, X.; Sun, X.; Zhang, J. Development of high-k hafnium–aluminum oxide dielectric films using sol–gel process. *J. Mater. Res.* **2014**, *29*, 1620-5. DOI
134. Sheng, J.; Lee, H. J.; Oh, S.; Park, J. S. Flexible and high-performance amorphous indium zinc oxide thin-film transistor using low-temperature atomic layer deposition. *ACS. Appl. Mater. Interfaces.* **2016**, *8*, 33821-8. DOI PubMed
135. Chen, X.; Zhang, G.; Wan, J.; et al. Transparent and flexible thin-film transistors with high performance prepared at ultralow temperatures by atomic layer deposition. *Adv. Electron. Mater.* **2019**, *5*, 1800583. DOI

136. Sheng, J.; Hong, T.; Lee, H. M.; et al. Amorphous IGZO TFT with high mobility of ~70 cm^2/(V s) via vertical dimension control using PEALD. *ACS. Appl. Mater. Interfaces.* **2019**, *11*, 40300-9. DOI PubMed
137. Jo, J. W.; Kim, Y. H.; Park, J.; et al. Ultralow-temperature solution-processed aluminum oxide dielectrics via local structure control of nanoclusters. *ACS. Appl. Mater. Interfaces.* **2017**, *9*, 35114-24. DOI PubMed
138. Hsu, H.; Chang, C.; Cheng, C. Room-temperature flexible thin film transistor with high mobility. *Curr. Appl. Phys.* **2013**, *13*, 1459-62. DOI
139. Hsu, H.; Chang, C.; Cheng, C. A flexible IGZO thin-film transistor with stacked TiO_2-based dielectrics fabricated at room temperature. *IEEE. Electron. Device. Lett.* **2013**, *34*, 768-70. DOI
140. Jo, J. W.; Kim, K. H.; Kim, J.; Ban, S. G.; Kim, Y. H.; Park, S. K. High-mobility and hysteresis-free flexible oxide thin-film transistors and circuits by using bilayer sol-gel gate dielectrics. *ACS. Appl. Mater. Interfaces.* **2018**, *10*, 2679-87. DOI PubMed
141. Yang, W.; Song, K.; Jung, Y.; Jeong, S.; Moon, J. Solution-deposited Zr-doped AlO*x* gate dielectrics enabling high-performance flexible transparent thin film transistors. *J. Mater. Chem. C.* **2013**, *1*, 4275-82. DOI
142. Xiao, P.; Dong, T.; Lan, L.; et al. High-mobility flexible thin-film transistors with a low-temperature zirconium-doped indium oxide channel layer. *Phys. Status. Solidi. RRL.* **2016**, *10*, 493-7. DOI
143. Jo, J. W.; Kim, J.; Kim, K. T.; et al. Highly stable and imperceptible electronics utilizing photoactivated heterogeneous sol-gel metal-oxide dielectrics and semiconductors. *Adv. Mater.* **2015**, *27*, 1182-8. DOI PubMed
144. Kim, H.; Kim, T.; Kang, Y.; et al. Sub-volt metal-oxide thin-film transistors enabled by solution-processed high-*k* Gd-doped HfO_2 dielectric films. *Mat. Sci. Semicon. Proc.* **2023**, *166*, 107746. DOI
145. Kim, J.; Choi, S.; Jo, J.; Park, S. K.; Kim, Y. Solution-processed lanthanum-doped Al_2O_3 gate dielectrics for high-mobility metal-oxide thin-film transistors. *Thin. Solid. Films.* **2018**, *660*, 814-8. DOI
146. Kim, J.; Kim, M.; Kang, Y.; et al. Photoactivated high-k lanthanum oxide-aluminum oxide (La_2O_3–Al_2O_3) alloy-type gate dielectrics for low-voltage-operating flexible transistors. *J. Alloys. Compd.* **2020**, *842*, 155671. DOI
147. Zhu, Y.; Liu, G.; Xin, Z.; Fu, C.; Wan, Q.; Shan, F. Solution-processed, electrolyte-gated In_2O_3 flexible synaptic transistors for brain-inspired neuromorphic applications. *ACS. Appl. Mater. Interfaces.* **2020**, *12*, 1061-8. DOI PubMed
148. Samanta, C.; Ghimire, R. R.; Ghosh, B. Fabrication of amorphous indium–gallium– zinc–oxide thin-film transistor on flexible substrate using a polymer electrolyte as gate dielectric. *IEEE. Trans. Electron. Devices.* **2018**, *65*, 2827-32. DOI
149. Hur, J. S.; Kim, J. O.; Kim, H. A.; Jeong, J. K. Stretchable polymer gate dielectric by ultraviolet-assisted hafnium oxide doping at low temperature for high-performance indium gallium tin oxide transistors. *ACS. Appl. Mater. Interfaces.* **2019**, *11*, 21675-85. DOI PubMed
150. Yu, M. C.; Ruan, D. B.; Liu, P. T.; et al. High performance transparent a-IGZO thin film transistors with ALD-HfO_2 gate insulator on colorless polyimide substrate. *IEEE. Trans. Nanotechnol.* **2020**, *19*, 481-5. DOI
151. Kim, C. Y.; Park, J. H.; Kim, T. G. Effect of photochemical hydrogen doping on the electrical properties of ZnO thin-film transistors. *J. Alloys. Compd.* **2018**, *732*, 300-5. DOI
152. Fernandes, C.; Santa, A.; Santos, Â.; et al. A sustainable approach to flexible electronics with zinc-tin oxide thin-film transistors. *Adv. Electron. Mater.* **2018**, *4*, 1800032. DOI
153. Abliz, A.; Wang, J.; Xu, L.; et al. Boost up the electrical performance of InGaZnO thin film transistors by inserting an ultrathin InGaZnO:H layer. *Appl. Phys. Lett.* **2016**, *108*, 213501. DOI
154. Kang, Y.; Ahn, B. D.; Song, J. H.; et al. Hydrogen bistability as the origin of photo-bias-thermal instabilities in amorphous oxide semiconductors. *Adv. Electron. Mater.* **2015**, *1*, 1400006. DOI
155. Wang, H.; He, J.; Xu, Y.; et al. Impact of hydrogen dopant incorporation on InGaZnO, ZnO and In_2O_3 thin film transistors. *Phys. Chem. Chem. Phys.* **2020**, *22*, 1591-7. DOI
156. Kang, B. H.; Kim, W. G.; Chung, J.; Lee, J. H.; Kim, H. J. Simple hydrogen plasma doping process of amorphous indium gallium zinc oxide-based phototransistors for visible light detection. *ACS. Appl. Mater. Interfaces.* **2018**, *10*, 7223-30. DOI PubMed
157. Abliz, A.; Gao, Q.; Wan, D.; et al. Effects of nitrogen and hydrogen codoping on the electrical performance and reliability of InGaZnO thin-film transistors. *ACS. Appl. Mater. Interfaces.* **2017**, *9*, 10798-804. DOI PubMed
158. Liu, P.; Chang, C.; Fuh, C.; Liao, Y.; Sze, S. M. Effects of nitrogen on amorphous nitrogenated InGaZnO (a-IGZO:N) thin film transistors. *J. Display. Technol.* **2016**, *12*, 1070-7. DOI
159. Xie, H.; Wu, Q.; Xu, L.; Zhang, L.; Liu, G.; Dong, C. Nitrogen-doped amorphous oxide semiconductor thin film transistors with double-stacked channel layers. *Appl. Surf. Sci.* **2016**, *387*, 237-43. DOI
160. Ding, X.; Yang, J.; Qin, C.; Yang, X.; Ding, T.; Zhang, J. Nitrogen-doped ZnO film fabricated via rapid low-temperature atomic layer deposition for high-performance ZnON transistors. *IEEE. Trans. Electron. Devices.* **2018**, *65*, 3283-90. DOI
161. Kim, D. G.; Choi, H.; Kim, Y. S.; et al. Selectively nitrogen doped ALD-IGZO TFTs with extremely high mobility and reliability. *ACS. Appl. Mater. Interfaces.* **2023**, *15*, 31652-63. DOI PubMed
162. Seo, J. S.; Jeon, J. H.; Hwang, Y. H.; et al. Solution-processed flexible fluorine-doped indium zinc oxide thin-film transistors fabricated on plastic film at low temperature. *Sci. Rep.* **2013**, *3*, 2085. DOI PubMed PMC
163. Saha, J. K.; Ali, A.; Bukke, R. N.; Kim, Y. G.; Islam, M. M.; Jang, J. Performance improvement for spray-coated ZnO TFT by F doping with spray-coated Zr–Al–O gate insulator. *IEEE. Trans. Electron. Devices.* **2021**, *68*, 1063-9. DOI
164. Yin, X.; Chen, Y.; Li, G.; et al. Analysis of low frequency noise in *in situ* fluorine-doped ZnSnO thin-film transistors. *AIP. Advances.* **2021**, *11*, 045326. DOI

165. Ruan, D.; Liu, P.; Chiu, Y.; et al. Performance improvements of tungsten and zinc doped indium oxide thin film transistor by fluorine based double plasma treatment with a high-K gate dielectric. *Thin. Solid. Films.* **2018**, *665*, 117-22. DOI
166. Yin, X.; Lin, D.; Zhong, W.; et al. In-situ fluorine-doped ZnSnO thin film and thin-film transistor. *Solid. State. Electron.* **2023**, *208*, 108726. DOI
167. Qian, L. X.; Lai, P. T. Fluorinated InGaZnO thin-film transistor with HfLaO gate dielectric. *IEEE. Electron. Device. Lett.* **2014**, *35*, 363-5. DOI
168. Miyakawa, M.; Nakata, M.; Tsuji, H.; Iino, H.; Fujisaki, Y. Impact of fluorine doping on solution-processed In–Ga–Zn–O thin-film transistors using an efficient aqueous route. *AIP. Advances.* **2020**, *10*, 065004. DOI
169. Hanyu, Y.; Domen, K.; Nomura, K.; et al. Hydrogen passivation of electron trap in amorphous In-Ga-Zn-O thin-film transistors. *Appl. Phys. Lett.* **2013**, *103*, 202114. DOI
170. Gaspar, D.; Pereira, L.; Gehrke, K.; Galler, B.; Fortunato, E.; Martins, R. High mobility hydrogenated zinc oxide thin films. *Sol. Energy. Mat. Solar. C.* **2017**, *163*, 255-62. DOI
171. Tsao, S.; Chang, T.; Huang, S.; et al. Hydrogen-induced improvements in electrical characteristics of a-IGZO thin-film transistors. *Solid. State. Electron.* **2010**, *54*, 1497-9. DOI
172. Kim, H. J.; Park, S. Y.; Jung, H. Y.; et al. Role of incorporated hydrogen on performance and photo-bias instability of indium gallium zinc oxide thin film transistors. *J. Phys. D. Appl. Phys.* **2013**, *46*, 055104. DOI
173. Li, J.; Ju, S.; Tang, Y.; et al. Remarkable bias-stress stability of ultrathin atomic-layer-deposited indium oxide thin-film transistors enabled by plasma fluorination. *Adv. Funct. Mater.* **2024**, *34*, 2401170. DOI
174. Kim, D.; Yoo, K. S.; Kim, H.; Park, J. Impact of N_2O plasma reactant on PEALD-SiO_2 insulator for remarkably reliable ALD-oxide semiconductor TFTs. *IEEE. Trans. Electron. Devices.* **2022**, *69*, 3199-205. DOI
175. Raja, J.; Jang, K.; Balaji, N.; choi, W.; Thuy, T. T.; Yi, J. Negative gate-bias temperature stability of N-doped InGaZnO active-layer thin-film transistors. *Appl. Phys. Lett.* **2013**, *102*, 083505. DOI
176. Han, Y.; Yan, H.; Tsai, Y.; Li, Y.; Zhang, Q.; Shieh, H. D. Influences of nitrogen doping on the electrical characteristics of indium-zinc-oxide thin film transistors. *IEEE. Trans. Device. Mater. Relib.* **2016**, *16*, 642-6. DOI
177. Yu, X.; Zhou, N.; Smith, J.; et al. Synergistic approach to high-performance oxide thin film transistors using a bilayer channel architecture. *ACS. Appl. Mater. Interfaces.* **2013**, *5*, 7983-8. DOI PubMed
178. Song, J. H.; Kim, K. S.; Mo, Y. G.; Choi, R.; Jeong, J. K. Achieving high field-effect mobility exceeding 50 cm^2/Vs in In-Zn-Sn-O thin-film transistors. *IEEE. Electron. Device. Lett.* **2014**, *35*, 853-5. DOI
179. Baptista, A.; Silva, F.; Porteiro, J.; Míguez, J.; Pinto, G. Sputtering physical vapour deposition (PVD) coatings: a critical review on process improvement and market trend demands. *Coatings* **2018**, *8*, 402. DOI
180. Liu, J.; Buchholz, D. B.; Chang, R. P. H.; Facchetti, A.; Marks, T. J. High-performance flexible transparent thin-film transistors using a hybrid gate dielectric and an amorphous zinc indium tin oxide channel. *Adv. Mater.* **2010**, *22*, 2333-7. DOI PubMed
181. Bao, Q.; Chen, C.; Wang, D.; Ji, Q.; Lei, T. Pulsed laser deposition and its current research status in preparing hydroxyapatite thin films. *Appl. Surf. Sci.* **2005**, *252*, 1538-44. DOI
182. Ogugua, S. N.; Ntwaeaborwa, O. M.; Swart, H. C. Latest development on pulsed laser deposited thin films for advanced luminescence applications. *Coatings* **2020**, *10*, 1078. DOI
183. Johnson, R. W.; Hultqvist, A.; Bent, S. F. A brief review of atomic layer deposition: from fundamentals to applications. *Mater. Today.* **2014**, *17*, 236-46. DOI
184. Bubel, S.; Meyer, S.; Kunze, F.; Chabinyc, M. L. Ionic liquid gating reveals trap-filled limit mobility in low temperature amorphous zinc oxide. *Appl. Phys. Lett.* **2013**, *103*, 152102. DOI
185. Wilson, S. K.; Hunt, R.; Duffy, B. R. The rate of spreading in spin coating. *J. Fluid. Mech.* **2000**, *413*, 65-88. DOI
186. Habibi, M.; Rahimzadeh, A.; Bennouna, I.; Eslamian, M. Defect-free large-area (25 cm^2) light absorbing perovskite thin films made by spray coating. *Coatings* **2017**, *7*, 42. DOI
187. Goh, G. L.; Zhang, H.; Chong, T. H.; Yeong, W. Y. 3D printing of multilayered and multimaterial electronics: a review. *Adv. Electron. Mater.* **2021**, *7*, 2100445. DOI
188. Huang, K.; Cai, X.; Shang, R.; et al. Printed high-adhesion flexible electrodes based on an interlocking structure for self-powered intelligent movement monitoring. *ACS. Appl. Mater. Interfaces.* **2023**, *15*, 58583-92. DOI PubMed
189. Tan, H. W.; Choong, Y. Y. C.; Kuo, C. N.; Low, H. Y.; Chua, C. K. 3D printed electronics: processes, materials and future trends. *Prog. Mater. Sci.* **2022**, *127*, 100945. DOI
190. Park, Y. G.; Yun, I.; Chung, W. G.; Park, W.; Lee, D. H.; Park, J. U. High-resolution 3D printing for electronics. *Adv. Sci.* **2022**, *9*, e2104623. DOI PubMed PMC
191. Kim, D. H.; Song, J.; Choi, W. M.; et al. Materials and noncoplanar mesh designs for integrated circuits with linear elastic responses to extreme mechanical deformations. *Proc. Natl. Acad. Sci. U. S. A.* **2008**, *105*, 18675-80. DOI
192. Rockett, A. Semiconductor alloys. In: The materials science of semiconductors. Springer; 2007. pp. 245-268. DOI
193. Park, C. B.; Na, H.; Yoo, S. S.; Park, K. Electrical characteristics of a-IGZO transistors along the in-plane axis during outward bending. *Microelectron. Reliab.* **2016**, *59*, 37-43. DOI
194. Dou, W.; Tan, Y. Junctionless dual in-plane-gate thin-film transistors with AND logic function on paper substrates. *ACS. Omega.* **2019**, *4*, 21417-20. DOI PubMed PMC
195. Guo, J.; Liu, J.; Yang, B.; et al. Biodegradable junctionless transistors with extremely simple structure. *IEEE. Electron. Device. Lett.*

2015, *36*, 908-10. DOI

196. Baruah, R. K.; Paily, R. P. High-temperature effects on device performance of a junctionless transistor. In: 2012 International Conference on Emerging Electronics; 2012 Dec 15-17; Mumbai, India. IEEE; 2012. p. 1-4. DOI
197. Jiang, J.; Sun, J.; Dou, W.; Zhou, B.; Wan, Q. Junctionless in-plane-gate transparent thin-film transistors. *Appl. Phys. Lett.* **2011**, *99*, 193502. DOI
198. Jeon, S. P.; Jo, J. W.; Nam, D.; Kang, D. W.; Kim, Y. H.; Park, S. K. Junctionless structure indium-tin oxide thin-film transistors enabling enhanced mechanical and contact stability. *ACS. Appl. Mater. Interfaces.* **2024**, *16*, 38198-207. DOI PubMed
199. Miyakawa, M.; Tsuji, H.; Nakata, M. Highly stretchable island-structure metal oxide thin-film transistor arrays using acrylic adhesive for deformable display applications. *J. Soc. Info. Display.* **2022**, *30*, 699-705. DOI
200. Nakata, M.; Motomura, G.; Nakajima, Y.; et al. Development of flexible displays using back-channel-etched In-Sn-Zn-O thin-film transistors and air-stable inverted organic light-emitting diodes: flexible displays using BCE-ITZO-TFTs and iOLEDs. *Jnl. Soc. Info. Display.* **2016**, *24*, 3-11. DOI
201. Xu, H.; Luo, D.; Li, M.; et al. A flexible AMOLED display on the PEN substrate driven by oxide thin-film transistors using anodized aluminium oxide as dielectric. *J. Mater. Chem. C.* **2014**, *2*, 1255-9. DOI